

Responses of field-grown maize to different soil types, water regimes, and contrasting vapor pressure deficit

Thuy Huu Nguyen¹, Thomas Gaiser¹, Jan Vanderborcht³, Andrea Schnepf³, Felix Bauer³, Anja Klotzsche³, Lena Lärm³, Hubert Hüging¹, Frank Ewert^{1, 2}

¹University of Bonn, Institute of Crop Science and Resource Conservation (INRES), Katzenburgweg 5, 53115 Bonn, Germany

²Leibniz Centre for Agricultural Landscape Research (ZALF), Institute of Landscape Systems Analysis, Eberswalder Strasse 84, 15374 Muencheberg, Germany

³Agrosphere (IBG-3), Institute of Bio- and Geosciences, Forschungszentrum Jülich GmbH, 52428, Jülich, Germany

*Corresponding author, email: tngu@uni-bonn.de

Abstracts

Drought is a serious constraint to crop growth and production of important staple crops such as maize. Improved understanding of the responses of crops to drought can be incorporated into cropping system models to support crop breeding, varietal selection and management decisions for minimizing negative impacts. We investigate the impacts of different soil types (stony and silty) and water regimes (irrigated and rainfed) on hydraulic linkages between soil and plant, as well as root: shoot growth characteristics. Our analysis is based on a comprehensive dataset measured along the soil-plant-atmosphere pathway at field scale in two growing seasons (2017, 2018) with contrasting climatic conditions (low and high VPD). Roots were observed mostly in the topsoil (10-20 cm) of the stony soil while more roots were found in the subsoil (60-80 cm) of the silty soil. The difference in root length was pronounced at silking and harvest between the soil types. Total root length was 2.5 - 6 times higher in the silty soil compared to the stony soil with the same water treatment. At silking time, the ratios of root length to shoot biomass in the rainfed

24 plot of the silty soil (F2P2) were 3 times higher than those in the irrigated silty soil (F2P3) while the ratio
25 was similar for two water treatments in the stony soil. With the same water treatment, the ratios of root
26 length to shoot biomass of silty soil was higher than stony soil. The observed minimum leaf water potential
27 (ψ_{leaf}) varied from around -1.5 MPa in the rainfed plot in 2017 to around -2.5 MPa in the same plot of the
28 stony soil in 2018. In the rainfed plot, the minimum ψ_{leaf} in the stony soil was lower than in silty soil from
29 -2 to -1.5 MPa in 2017, respectively while these were from -2.5 to -2 MPa in 2018, respectively. Leaf water
30 potential, water potential gradients from soil to plant roots, plant hydraulic conductance ($K_{\text{soil_plant}}$),
31 stomatal conductance, transpiration, and photosynthesis were considerably modulated by the soil water
32 content and the conductivity of the rhizosphere. When the stony soil and silt soil are compared, the higher
33 'stress' due to the lower water availability in the stony soil resulted in less roots with a higher root tissue
34 conductance in the soil with more stress. When comparing the rainfed with the irrigated plot in the silty
35 soil, the higher stress in the rainfed soil resulted in more roots with a lower root tissue conductance in the
36 treatment with more stress. This illustrates that the 'response' to stress can be completely opposite
37 depending on conditions or treatments that lead to the differences in stress that are compared. To respond
38 to water deficit, maize had higher water uptake rate per unit root length and higher root segment
39 conductance in the stony soil than in the silty soil, while the crop reduced transpired water via reduced
40 aboveground plant size. Future improvements of soil-crop models in simulating gas exchange and crop
41 growth should further emphasize the role of soil textures on stomatal function, dynamic root growth, and
42 plant hydraulic system together with aboveground leaf area adjustments.

43 **Key words:** irrigation, plant hydraulic conductance, transpiration, root length, soil types, soil to leaf water
44 potential, stomatal regulation

45 **Abbreviations:** DOY: day of the year; DAS: day after sowing; TUE: transpiration use efficiency; SF: sap flow;
46 LAI: green leaf area index; PAR: photosynthetically active radiation; VPD: vapor pressure deficit; An: net
47 leaf photosynthesis; E: leaf transpiration; ψ_{leaf} : leaf water potential; $\psi_{\text{sunlitleaf}}$: leaf water potential of sunlit

48 leaf; $\psi_{\text{shadedleaf}}$: leaf water potential of shaded leaf; K_{soil} : hydraulic conductance of soil; K_{root} : root hydraulic
49 conductance; K_{stem} : stem hydraulic conductance; $\psi_{\text{soil_effec}}$: effective soil water potential; $\psi_{\text{difference}}$:
50 difference between effective soil water potential and sunlit leaf water potential; $K_{\text{soil_root}}$: root system
51 hydraulic conductance (includes soil and root hydraulic conductance); $K_{\text{soil_plant}}$: whole plant hydraulic
52 conductance (includes below and aboveground components).

53 **1. Introduction**

54 Maize (*Zea mays L.*) is a major staple crop throughout the world. Drought stress, which negatively affects
55 crop growth and yield, is of increasing concern in several important maize cultivating regions (Daryanto et
56 al., 2016). Increases in frequency and severity of drought events due to climate change have been recently
57 reported (IPCC, 2022). Thus, field observations and understanding on how maize responds to water stress
58 are necessary to suggest promising traits for breeding programs (Vadez et al., 2021) as well as irrigation
59 schemes (Fang and Su, 2019; Q. Cai et al., 2017). Improved understanding of crops' response to drought
60 can be incorporated into soil-crop models (e.g. crop modelling and soil-vegetation-atmosphere transfer
61 modelling).

62 Stomatal regulation is often considered as a key aboveground hydraulic variable in regulating water use
63 of crops. Maize was considered as isohydric plant in which stomata are closed in response to sensing
64 drought conditions to maintain leaf water potential (ψ_{leaf}) above critical levels ($\psi_{\text{threshold}}$ or minimum ψ_{leaf})
65 (Tardieu and Simonneau, 1998). Investigations of how stomatal controls differ among species and
66 genotypes commonly observed minimum ψ_{leaf} or analyzed genetic variability of stomatal control in
67 response to varying soil water content. Analyzing measurements of ψ_{leaf} from 400 lines of maize of tropical
68 and European origins under greenhouse and growth chamber conditions, Welcker et al. (2011) reported
69 values of minimum ψ_{leaf} from -0.8 to -1.5 MPa, indicating genetic variability of stomatal responses. The
70 isohydric behavior is due to different mechanisms including hydraulic and/or chemical (e.g. abscisic acid
71 [ABA]) signals (Tardieu, 2016). The degree to which these underlying mechanisms interact and differ

72 among genotypes and/or environmental scenarios in explaining the stomatal regulation is still debated
73 (Tardieu, 2016, Hochberg et al., 2018). Field evidence in variation of the minimum ψ_{leaf} of maize due to soil
74 water availability is rarely reported.

75 Water flow along the soil-plant-atmosphere continuum is determined by a series of hydraulic
76 conductivities and gradients in water potential. Hydraulic conductance of soil (K_{soil}), root hydraulic
77 conductance (K_{root}), and stem hydraulic conductance (K_{stem}) determine water potential from soil to root
78 and root xylem water, and thus magnitude of ψ_{leaf} . There are two main resistances to water flow from the
79 soil to the shoot, namely the soil and the root resistances, often expressed as their inverse, K_{soil} and K_{root}
80 (Nguyen et al., 2020; Cai et al., 2018). In wet soils, the soil hydraulic conductivity is much higher than that
81 of roots, and water flow is mainly controlled by root hydraulic conductivity (Hopmans and Bristow, 2002;
82 Draye et al., 2010). It is well-known that a decrease in soil matric potential and soil hydraulic conductivity
83 triggers stomatal closure and thus results in reduction in transpiration rate (Sinclair and Ludlow, 1986;
84 Carminati and Javaux 2020; Abdalla et al., 2021). For the root water uptake and controlling stomata, the
85 location where soil and roots are in close contact (rhizosphere) is most important, because when this thin
86 layer of rhizosphere is disconnected (i.e. soil-root contact is lost), the water movement from soil toward
87 the roots is reduced, which might trigger stomatal closure to maintain hydraulic integrity of plant
88 (Carminati et al., 2016; Rodriguez-Dominguez and Brodribb, 2019; Abdalla et al., 2022). The magnitude of
89 the drop of water potential between bulk soil and soil-root interface increases considerably at different
90 levels of soil dryness for different soil types (Carminati and Javaux, 2020; Abdalla et al., 2022). Hydraulic
91 limits in the soil (Carminati and Javaux, 2020), or in the root-soil interface [as measured for olive trees by
92 Rodriguez-Dominguez and Brodribb, 2019 or tomato (Abdalla et al., 2022)], or in the root properties
93 (Bourbia et al., 2021; Cai et al., 2022; Nguyen et al., 2020; Cai et al., 2018) or due to both soil textures and
94 root phenotypes (Cai et al., 2022b) emphasized the importance of belowground hydraulics (Carminati and
95 Javaux, 2020). However, also the shoot hydraulic conductance could be limiting in some crop plants

96 (Gallardo et al., 1996) or in trees (Domec and Pruyn, 2008; Tsuda and Tyree, 1997). Stomatal conductance
97 and shoot hydraulic conductance showed close links to each other in pine trees (Hubbard et al., 2001).
98 This summary illustrates three points: (i) current studies have often focused either on above or on below
99 hydraulic limits, but rarely consider both (ii) it is unclear the roles and relations of soil hydraulic properties
100 to root and plant hydraulic conductance (thus influences on stomatal conductance) (iii) the role of different
101 hydraulic processes across the soil - plant - atmosphere continuum i.e. soil to roots, stem, and soil-plant
102 hydraulic conductance in controlling stomatal conductance remains unclear.

103 Simultaneous measurements of atmospheric conditions (light intensity and vapor pressure deficit), leaf
104 water potential, and transpiration rates, coupled with measurements of root, stem and whole soil-plant
105 hydraulic conductance, root architecture, and soil water potential distribution could reveal the relative
106 importance of rhizosphere, shoot and root growth, and hydraulic conductance vulnerability, especially
107 under progressive soil drying at field conditions (Carminati and Javaux, 2020; Tardieu et al., 2017). For the
108 soil water conditions, soil texture and hydraulic characteristics are very important because they influence
109 soil water movement and thus affect infiltration, surface and sub-surface runoff, and ultimately plant
110 available soil water (Vereecken et al., 2016). Soil texture properties, characterized by different fractions of
111 clay, silt, and sand particles, are important drivers in determining the soil water retention properties
112 (Scharwies and Dinneny, 2019; Stadler et al., 2015; Zhuang et al., 2001). Soil with higher water holding
113 capacity (here the silty soil with low stone content) have a larger amount of plant available water which in
114 turn enables crops to better meet the evaporative demand and facilitates better crop growth as compared
115 to the soil with high stone content (Nguyen et al., 2020; Cai et al., 2018). Estimations of hydraulic
116 conductance (different organs and whole plant hydraulic conductance) were done for crop plants and
117 maize mainly under controlled environment or pot conditions e.g. for different species and genotypes
118 during soil drying (Sunita et al., 2014; Choudhary and Sinclair, 2014; Abdalla et al., 2022; Meunier et al.,
119 2018; Wang et al., 2017; Li et al., 2016) or various species and genotypes together with different soil

120 textures (Cai et al., 2022a), or soil texture with different vapor pressure deficit (VPD) (Cai et al., 2022b).
121 Compared to the substantial effect of soil texture, there was no evidence of an effect of VPD on both soil–
122 plant hydraulic conductance and on the relation between canopy stomatal conductance and soil–plant
123 hydraulic conductance in pot-grown maize (Cai et al., 2022b). Contrast results were found in winter wheat
124 where plant hydraulic conductance increased with rising VPD for some genotypes in wet conditions
125 (Ranawana et al., 2021). Vadez et al., (2021) examined the effects of soil types together with increasing
126 VPD on transpiration efficiency (TE) and yield under pot conditions for several C₄ species (maize, sorghum,
127 and millet). The interpretation of differences in TE was attributed to soil types, more specifically, to the
128 differences in soil hydraulic properties and soil hydraulic conductance. However, experimental evidence
129 linking root hydraulics to stomatal regulation was lacking in these two Vadez’s studies (Vadez et al., 2021).
130 Extrapolation and use of results obtained in pots or under greenhouse conditions to the field scale are
131 difficult due to the fact that soil substrates in pots might not represent natural soil in the field (Passioura,
132 2006). There is often greater evaporative demand and considerable fluctuation and interactions of climatic
133 variables in the field as compared to experiments under controlled or semi-controlled conditions. Recent
134 field studies have aimed at quantification of root hydraulic conductance and it’s linkages with crop growth
135 (leaf area and biomass) under different soil types (in wheat Cai et al., 2017; Cai et al., 2018; Nguyen et al.,
136 2020 or maize in Nguyen et al., 2022; Jorda et al., 2022). However, field studies that consider both below
137 (soil-root hydraulic conductance) and above (stem hydraulic conductance), or soil-plant hydraulic
138 conductance (including below and above-ground parts) and their roles in stomatal regulation as well as
139 crop growth (leaf area and biomass) are rarely carried out.

140 This study aims at further understanding of the hydraulic linkages between soil and plant and responses
141 of plants to drought stress in relation to root: shoot growth characteristics at field scale. We hypothesize
142 that, in field-grown maize, (1) soil-plant hydraulic conductance depends on soil hydraulic properties,
143 especially under dry soil conditions (2) minimum leaf water potential of maize is similar across soil types,

144 water treatments and climatic conditions. The hypotheses will be tested through three objectives: (i) to
145 investigate the effects of soil types, water application, and climatic condition on root growth and (ii) on
146 stomatal conductance, leaf photosynthesis, transpiration, leaf water potential, different components
147 of the hydraulic conductance (root, stem, and whole soil-plant), and (iii) to analyze the relative contribution
148 of root and shoot growth (leaf area and biomass) on the water uptake capacity of maize. These three
149 objectives will be achieved based on a comprehensive dataset covering the whole soil-plant continuum
150 over two growing maize seasons with contrasting climatic conditions (low and high VPD) under two water
151 treatments (rainfed and irrigated) and two different soil types (stony and silty soil).

152 **2. Materials and methods**

153 **2.1. Location and experimental set-up**

154 We carried out a field experiment at two rhizotron facilities in Selhausen, North Rhine-Westphalia,
155 Germany (50°52'N, 6°27'E). The field is slightly inclined with a maximum slope of around 4°. One rhizotrone
156 facility was located upslope (F1) with around 60% gravel by weight in the 10-cm topsoil while the second
157 rhizotrone facility was at downslope (F2) with silty soil (stone content is around 4% by weight).

158 Each rhizotrone facility was divided into three subplots of 7.25 m by 3.25 m: two rainfed plots (P1, P2),
159 and one irrigated plot (P3). In rainfed plots P1, other sowing densities and dates were used than in the
160 other plots and we excluded therefore these plots. Silage maize *cv.* Zoey was sown on 4 May and 8 May in
161 2017 and 2018, respectively, with a plant density of 10.66 seeds m⁻² (Figure 1a; Table 1). Detailed
162 information of crop management practices is provided in Table 1.

163 [Insert Table 1 here]

164 **2.2. Water applications**

165 Weather variables (global radiation, temperature, relative humidity, precipitation, and wind speed) were
166 recorded every 10 minutes by a nearby weather station (approx. 100 m from the experiment). Drip lines

167 (T-Tape 520-20-500, Wurzelwasser GbR, Müzenberg, Germany) were installed for irrigation at 0.3 m
168 intervals parallel to the crop rows. In 2017, maize received a total amount of 230 mm precipitation during
169 the growing period (136 days). Average, minimum and maximum daily air temperature were 17.6, 8.3, and
170 25.3 °C, respectively (Fig. 1b). The crop on P3 was irrigated (in total 130 mm) every 5-7 days (in total 10
171 times) using 13 mm of irrigation water per event between mid June to end of August for the irrigated plots
172 (2017F1P3 and 2017F2P3) (Fig. 1b). In 2018, average, minimum, and maximum daily air temperature were
173 19.2, 10.85, and 27.3 °C, respectively (Fig. 1b) and exceeded those of 2017. Characterized by exceptionally
174 hot and dry weather conditions, the summer season 2018 can be classified as an extreme year with respect
175 to plant growth at our experimental location. Maize experienced high temperatures and VPD, especially
176 around tasseling and silking. In 2018, only 91.3 mm of rain were recorded in the growing period of 2018
177 (107 days). The maize crop was irrigated every 5-7 days (in total 13 times), with a total amount of irrigation
178 of 257 mm and 239 mm between mid- June and mid- August for the irrigated plots 2018F1P3 and
179 2018F2P3, respectively (Fig. 1d). In contrast to 2017, the rainfed plot in the stony soil (2018F1P2) had to
180 be irrigated (in total 66 mm) four times (using 13, 22, 13, and 18 mm, respectively) to avoid a crop failure
181 due to severe drought (Fig. 1d).

182 [Insert Figure 1 here]

183 **2.3. Measurements**

184 **2.3.1. Soil water measurement and root growth**

185 At soil depths of 10, 20, 40, 60, 80, and 120 cm, MPS-2 matrix water potential and temperature sensors
186 (Decagon Devices Inc., UMS GmbH München, Germany) were installed to measure half-hourly soil water
187 potential and soil temperature. The range of the water potential measurements is from -9 kPa to
188 approximately -100000 kPa (pF 1.96 to pF 6.01). In addition to MPS-2, soil water potential was measured
189 by pressure transducer tensiometers (T4e, UMS GmbH, München, Germany) where the minimum

190 detectable suction is -85 kPa to +100 kPa. A detailed description of sensor installation, calibration and data
191 post processing can be found in Cai et al., (2016).

192 Minirhizotubes (7 m long clear acrylic glass tubes with outer and inner diameters of 6.4 and 5.6 cm,
193 respectively) were installed horizontally at six different depths of 10, 20, 40, 60, 80, and 120 cm below the
194 soil surface in each facility. There are three replicate tubes at each depth, accounting for 54 tubes in each
195 facility. Root measurements were taken manually by Bartz camera (Bartz Technology Corporation) (23
196 June 2017 – 12 September 2017) and VSI camera (Vienna Scientific Instruments GmbH) (08 June 2017 – 22
197 June 2017) in 2017 while only VSI was used in 2018 (23 May 2018 - 23 August 2018). Root images were
198 taken at 20 fixed positions from the left- and right-hand sides of each tube weekly (or biweekly) during the
199 growing seasons. The root images were analyzed by automated minirhizotube image analysis pipeline for
200 segmentation and automated feature extraction (Bauer et al., 2021). Two-dimensional root length density
201 (RLD, in units of cm cm^{-2}) was estimated from the total root length observed in the image and the image
202 surface area. The overview of camera system, minirhizotube images acquisition, and post-processing of
203 the root data were described in detail in Bauer et al. (2021) and Lärm et al., (2023).

204 **2.3.2. Crop growth measurement**

205 The phenology, plant height, stem diameter, green and brown leaf area, dry matter of different organs,
206 and total aboveground dry matter were observed and measured bi-weekly. Plant height was measured in
207 15 randomly selected plants. The diameters of five randomly selected stems were measured. Due to the
208 limited number of plants in each plot, only two plants per measurement date were sampled to determine
209 total aboveground dry matter and leaf area (7 and 8 times in 2017 and 2018, respectively). Green and
210 brown leaf area was measured by a LI-3100C (Licor Biosciences, Lincoln, Nebraska, USA). At harvest, five
211 separate replicates (1m^2 each) were harvested. The dry matter of separate organs was determined after
212 drying at $105\text{ }^\circ\text{C}$ for 48 hours (Nguyen et al., 2020).

213 **2.3.3. Leaf gas exchange, leaf water potential, and sap flow measurements**

214 Hourly leaf stomatal conductance (G_s), net photosynthesis (A_n), and leaf transpiration (E) were measured
215 every two weeks under clear sky conditions. Observations from 8 AM to 5 PM on four days and from 10
216 AM to 4 PM on six days were carried out in 2017. In 2018, measurements were carried out on 6 days from
217 8 AM to 7 PM and on 5 days from 10 AM to 4 PM (Nguyen et al., 2022a). The G_s , A_n , and E of two sunlit
218 leaves (uppermost fully developed leaves) and one shaded leaf of different plants were measured at
219 steady-state using a LICOR 6400 XT device (Licor Biosciences, Lincoln, Nebraska, USA). After leaf gas
220 exchange measurements, leaves were quickly detached using a sharp knife to measure leaf water potential
221 (ψ_{leaf}) with a digital pressure chamber (SKPM 140/ (40-50-80), Skye Instrument Ltd, UK) with the working
222 air pressure ranging from 0 to 35 bars. To study the diurnal course of ψ_{leaf} under dry and re-wetted soil
223 conditions, in 2018, measurements were undertaken for three additional days with predawn
224 measurements two days before and one day after irrigation. Further detail of measurement dates, range
225 of real time records of PAR, VPD and soil water status could be found in (Nguyen et al., 2022a).

226 In 2017 (from 7 July 2017 until harvest) and 2018 (from 28 June 2018 until harvest), 20 sap flow sensors
227 (SGA 13, SGB 16, and SGB 19 types) were installed (one sensor per plant and 5 maize plants per plot) based
228 on stem diameter size. Sensor data, in particular the partitioning of energy, electricity supply, sap flow,
229 and the temperature difference between upper and lower thermocouples (dT) of each sensor were
230 recorded at 10 minute intervals using a CR1000 data logger and two AM 16/32 multiplexers (Campbell
231 Scientific, Logan, Utah). The sap flow in the plant (g h^{-1}) was monitored directly by the data loggers
232 (Dynamax, 2007) and used as a surrogate for canopy transpiration based on the number of plants per
233 square meter.

234 **2.4. Calculation of total root length, root system conductance, stem, and whole plant hydraulic** 235 **conductance**

236 To estimate the total root length from minirhizotubes, we adopted the option 2 which was described in
 237 Cai et al., (2017). Total root length per square meter soil surface area within each soil layer ($m\ m^{-2}$) was
 238 computed by multiplying the root length density with the corresponding soil layer thickness. The root
 239 length density was determined in each depth by dividing the measured root length per minirhizotron
 240 image by the assumed volume the roots would have occupied in absence of the tube, i.e., $W * L * \text{tube}$
 241 radius (see Cai et al., 2017).

242 Following Nguyen et al., (2020), the effective soil water potential was calculated based on hourly measured
 243 soil water potential (ψ_i) and normalized root length density at six depths (10, 20, 40, 60, 80, and 120 cm)
 244 (NRLD_i), and soil layer thickness (Δz_i) in the soil profile (Equation 1).

$$\psi_{soil_effec} = \sum_{i=1}^N \psi_i NRLD_i \Delta z_i \quad (1)$$

245 We followed Ohm's law analogy by dividing the hourly sap flow by the difference between effective soil
 246 water potential and shaded leaf water potential to estimate root system conductance (K_{soil_root} - Equation
 247 2), between shaded leaf water potential and sunlit leaf water potential to estimate stem hydraulic
 248 conductance (K_{stem} - Equation 3), and between effective soil water potential and sunlit leaf water potential
 249 to estimate whole plant hydraulic conductance (K_{soil_plant} - Equation 4).

$$K_{soil_root} = Sapflow / (\psi_{soil_effec} - \psi_{shadedleaf}) \quad (2)$$

$$K_{stem} = Sapflow / (\psi_{shadedleaf} - \psi_{sunlitleaf}) \quad (3)$$

$$K_{soil_plant} = Sapflow / (\psi_{soil_effec} - \psi_{sunlitleaf}) \quad (4)$$

250 During one measurement day, four values of the K_{soil_root} , K_{stem} , and K_{soil_plant} were obtained from
 251 measurements between 11AM and 2 PM. The average and standard deviation of these hourly
 252 measurements were calculated for each measurement day in order to present the seasonal dynamics of
 253 those variables. To capture the diurnal and seasonal variations of sap flow and sunlit leaf water potential,

254 in addition, we plotted the hourly sap flow and hourly difference of effective soil water potential and sunlit
255 leaf water potential for three measurement days starting from predawn and whole seasons, respectively,
256 to derive the slope which is also $K_{\text{soil_plant}}$.

257 **2.5. Statistical analysis**

258
259 Regression analysis was performed to understand the relationship between the sap flow volume and the
260 difference of effective soil water potential and sunlit leaf water potential as well as the relationship
261 between the total aboveground biomass and cumulated water transpired (sap flow volume). These
262 analyses allow to derive the slope as proxy of $K_{\text{soil_plant}}$ and transpiration use efficiency, respectively. Since
263 all measured data have their own measurement errors, the generalized Deming regression was employed.
264 We performed relationships (via correlation coefficient and statistical significant levels) of midday leaf A_n ,
265 G_s , and E with midday K_{stem} , $K_{\text{soil_plant}}$, $K_{\text{soil_root}}$, sunlit leaf potential, $\psi_{\text{soil_effec}}$, and the difference of $\psi_{\text{soil_effec}}$
266 and sunlit leaf water potential ($\psi_{\text{difference}}$). All data processing and analysis were conducted using the R
267 statistical software (R Core Team, 2022).

268 **3. Results**

269 **3.1. Root growth under different water treatments, soil types and climatic conditions**

270 Observed root length (cm cm^{-2}) from the minirhizotubes in different soil depths at the first week of June
271 (stem elongation), around silking, and at harvest in two growing seasons are shown in the Figure 2. Root
272 length was similar among water treatments at the start of stem elongation in both years (Fig. 2a & 2d).
273 The difference in root length was pronounced at silking and harvest between the soil types. More root
274 growth was observed in the silty soil compared to the stony soil with the same water treatment (i.e. 2.5 -
275 6 times higher at depth 40 cm). This indicated the strong negative effects of stone content on root
276 development. In the stony soil, root length in the irrigated plot (F1P3) was slightly higher than in the rainfed
277 plot (F1P2). In contrast, the rainfed treatment (F2P2) in the silty soil showed much higher root length,
278 especially from 40 to 120 cm depths as compared to the irrigated plot (F2P3) in both growing seasons.

279 Much lower stone content and deep soil cracks in the silty soil (Morandage et al., 2021) allow root
280 extension to the subsoil, particularly in the rainfed plot F2P2. Root length in the rainfed treatment (F2P2)
281 in 2018, is higher than in 2017 which implies that root further developed to exploit the water in the soil
282 under the rainfed condition to meet the higher evaporative demand.

283 [Insert Figure 2 here]

284 Total root length (m m^{-2}) estimated from minirhizotubes and its ratio to shoot dry matter (m kg^{-1}) at three
285 measured dates (as in Figure 2) are shown in the Figure 3. Total root length was much higher for the silty
286 plots as compared to stony plots. In 2017, the highest total root length was observed in the rainfed plot of
287 the silty soil (F2P2) with approximately 9166 m m^{-2} and 9878 m m^{-2} around silking and harvest, respectively,
288 which was almost two times higher than in the irrigated plot (F2P3). These figures were higher in 2018
289 than 2017 where total root length of F2P2 was 10188 m m^{-2} and 13750 m m^{-2} at silking and harvest time,
290 respectively. For the rainfed stony soil (F1P2), soil water depletion around the beginning of June in 2017
291 (Supplementary material 1a) and from the first two weeks of June to harvest in 2018 (Supplementary
292 material 2a) caused the strong reduction of shoot biomass. In the stony soil, the shoot dry matter of the
293 irrigated plot (F1P3) and the rainfed plot (F1P2) were 1275 and 536 g m^{-2} at silking time (e.g. 19 July 2018
294 – DOY 200, Supplementary material 3a and 3b). However, there was a minor difference between F1P2 and
295 F1P3 in terms of the ratio of root length to shoot dry matter. In the silty soil, a decrease of soil water
296 potential was not pronounced (compared to stony soil) in both years 2017 and 2018 (Supplementary
297 material 1b and 2b). In 2018, shoot biomass in the irrigated stony soil (F1P3) and silt soil (F2P3) were
298 similar (1275 and 1299 g m^{-2} , respectively on 19 July 2018 – DOY 200) while the shoot biomass of the
299 rainfed silty soil (F2P2) was 876 g m^{-2} (Supplementary material 3a & 3b). However, the ratios of root length
300 to shoot biomass in the rainfed plot of the silty soil (F2P2) were 3 and 6 times higher than those in the
301 irrigated silty soil (F2P3) and stony soil (F1P3), respectively (e.g. 18 July, DOY 199). Moreover, total root
302 length was relatively equal among treatments at the start of set elongation (8 June - DOY 159) in both

303 years, while this was the opposite for the ratio of root length to shoot dry matter. This firstly illustrated
304 that the finer soil texture without stones and with soil cracks could favor the root growth which indicates
305 strong interactions of root and soil conditions. Secondly, the larger root length and higher atmospheric
306 evaporative demand in 2018 than 2017 indicates also the interaction of root growth and climatic
307 conditions.

308 [Insert Figure 3 here]

309 **3.2. Stomatal conductance, photosynthesis, transpiration, and K_{soil_plant}**

310 **3.2.1. Diurnal course of stomatal conductance, photosynthesis, transpiration, and water potential at leaf** 311 **level**

312 After a long period with high temperatures and no rainfall, soil water reduction in the rainfed plot of the
313 stony soil (F1P2) on 17 July 2018 (Supplementary material 2) resulted in three times lower net
314 photosynthesis (A_n), stomatal conductance (G_s), transpiration (E) and leaf water potential (ψ_{leaf}) as
315 compared to the remaining treatments (Fig. 4). This indicates that the soil water content strongly affected
316 the stomatal conductance. Stomatal closure was much pronounced around midday in F1P2 while this was
317 not the case in the F2P2, indicating the soil type strongly affected the stomatal conductance and leaf gas
318 exchange.

319 [Insert Figure 4 here]

320 Leaf gas exchange and leaf water potential in the F1P2 were still much lower than in other plots (Figure
321 5). On 18 July 2018, after application of 22.75 mm of irrigation water (at 4 PM), photosynthesis, stomatal
322 conductance, transpiration and leaf water potential were slightly increased in F1P2. However, these were
323 still smaller than in F2P2 and the two irrigated plots.

324 [Insert Figure 5 here]

325 On the next day after irrigation, leaf gas exchange and water potential were considerably increased in the
326 F1P2 (Figure 6). Leaf curling was also less pronounced as compared the two previous days. This indicated
327 the recovery of plant after watering. Leaf water potential, photosynthesis, stomatal conductance, and leaf
328 transpiration were almost similar to other plots from predawn throughout the day.

329 [Insert Figure 6 here]

330 **3.2.2. Seasonal course of stomatal conductance, photosynthesis, transpiration, water potential, and** 331 **plant hydraulic conductance at the leaf level**

332 Seasonal stomatal conductance (G_s) and leaf water potential (ψ_{leaf}) are described in Figure 7. The
333 relationship between two variables was rather noisy and non-linear. The leaf water potential showed
334 distinct patterns among treatments in one growing season. Minimum ψ_{leaf} was maintained at around -1.5
335 MPa in the irrigated plot in stony soil (F1P3) and two plots in the silty soil (F2P2 and F2P3). Lower minimum
336 ψ_{leaf} could be observed in the rainfed plot with stony soil (F1P2) but it did not go beyond -2 MPa. Minor
337 leaf curling was observed only in the second week of June in the F1P2 in 2017. In 2018, the higher
338 temperature and vapor pressure deficit resulted in lower minimum ψ_{leaf} in all treatments and soil types as
339 compared to 2017. The minimum ψ_{leaf} was around -2 MPa in F1P3, F2P2, and F2P3 while ψ_{leaf} could drop
340 below -2 MPa in F1P2 which was due to the severe soil water deficit. The low G_s and ψ_{leaf} associated with
341 measurement dates when the substantial leaf curling was observed at mid of July to the end of growing
342 season in F1P2 in 2018 (Supplementary material 3c & 3d and Supplementary material 4c & d).

343 [Insert Figure 7 here]

344 The effective soil water potential ($\psi_{\text{soil_effect MD}}$), sunlit leaf water potential ($\psi_{\text{sunlitleaf MD}}$), stomatal
345 conductance (G_{SMD}), and whole plant hydraulic conductance ($K_{\text{soil_plant MD}}$) at midday at several times during
346 the growing season are presented in Figures 8 and 9 for 2017 and 2018, respectively. As expected, there
347 was not much difference in terms of $\psi_{\text{soil_effecMD}}$ among F1P3, F2P2, and F2P3 from 02 August to one week

348 before harvest in 2017. The lowest $\psi_{\text{soil_effec MD}}$ was observed in the F1P2. Leaf water potential dropped
349 drastically but also $K_{\text{soil_plant MD}}$ increased strongly whereas $\psi_{\text{soil_effec MD}}$ remained quite similar (e.g. 18 July).
350 This is because sap flow have increased substantially in this day (e.g. from 2.34 mm d⁻¹ on 17 July to 6.97
351 mm d⁻¹ on 18 July for the F1P2). The stomatal conductance decreased a lot in this day which could be
352 explained that the atmospheric demand increased (e.g. global radiation was 13.6 MJ m⁻² on 17 July
353 compared to 23.9 MJ on 18 July while daily VPD was 0.7 kPa and 1.2 kPa, respectively) even more than the
354 sap flow. Midday sunlit leaf water potential was not distinctively different among treatments with the
355 lowest $\psi_{\text{sunlitleaf MD}}$ around -1.6 MPa throughout season. Also, G_{SMD} was rather similar among plots. The
356 $K_{\text{soil_plant MD}}$ ranged from 0.125 to 0.96 mm h⁻¹ MPa⁻¹ with a sharp reduction before harvest. In general, the
357 lowest values of $K_{\text{soil_plant MD}}$ were found in F1P2 which was consistent with the smaller overall seasonal
358 $K_{\text{soil_plant}}$ (as the slope of linear relationship between sap flow and difference of effective soil water potential
359 and sunlit leaf water potential) (see Supplementary material 5).

360 [Insert Figure 8 here]

361 The $\psi_{\text{soil_effec MD}}$ was substantially different in the two soil types and water treatments in 2018 (Figure 9a).
362 Both F1P2 and F1P3 showed a gradual drop of $\psi_{\text{soil_effec MD}}$ from 15 June until the third week of July then
363 increased after irrigation events on 18 July (Supplementary material 2b). However, $\psi_{\text{soil_effec MD}}$ of F1P2 was
364 much lower than F1P3 toward the harvest. The $\psi_{\text{soil_effec MD}}$ of F2P2 and F2P3 only decreased progressively
365 from around 10 July till harvest even though there was water supply from the irrigation (Supplementary
366 material 2b). The water applied by irrigation and coming in by rainfall were insufficient to wet up the
367 deeper soil layers which remained dry. The low G_{SMD} was corresponding to the lowest $\psi_{\text{sunlitleaf MD}}$ and
368 $K_{\text{soil_plant MD}}$ from the F1P2 (Figure 9c & 9d). The $K_{\text{soil_plant MD}}$ from all plots was ranging from 0.12 to 0.91 mm
369 h⁻¹ MPa⁻¹. There was the drop in $K_{\text{soil_plant MD}}$ (i.e. 3 to 9 July or 17-18 July) before irrigation in this plot.
370 However, it increased after the irrigation (i.e. 10 July and 19 July). This suggests that $K_{\text{soil_plant}}$ depends
371 strongly on the soil water content and the conductivity of the rhizosphere.

372 [Insert Figure 9 here]

373 **3.2.3. Relationships of stomatal conductance, transpiration, photosynthesis with plant hydraulic**
374 **variables at the plant canopy level**

375 The slope of linear relationship between sap flow and difference of $\psi_{\text{soil_effec}}$ and $\psi_{\text{sunlitleaf}}$ is shown for three
376 consecutive days (leaf water potential measurements from the predawn) and before and after irrigation
377 applications (17, 18, and 19 July 2018) (Figure 10). On both dates 17 and 18 July, the difference between
378 $\psi_{\text{soil_effec}}$ and $\psi_{\text{sunlitleaf}}$ was around -1.6 MPa with very low transpiration rates in the treatment F1P2 which
379 was associated with very low plant hydraulic conductance and leaf curling. The whole plant hydraulic
380 conductance was disrupted on these two days (0.06 and 0.16 $\text{mm h}^{-1} \text{MPa}^{-1}$ for 17 and 18 July, respectively).
381 Water was supplied on 18 July at 1 PM for the irrigated plots (F1P3, F2P3) as well as F1P2 at 4 PM (for
382 saving plant from death due to severe drought stress). $K_{\text{soil_plant}}$ was slightly changed (0.43 and 0.57 mm h^{-1}
383 MPa^{-1} for F1P3 on 18 and 19 July, respectively and 0.5 and 0.58 $\text{mm h}^{-1} \text{MPa}^{-1}$ for F2P3 on 18 and 19 July,
384 respectively). However, the increase of $K_{\text{soil_plant}}$ was substantial in the F1P2 after the irrigation. Soil water
385 replenishment and an increase in the root - soil contact (Fig. 9a) allowed the $K_{\text{soil_plant}}$ to recover overnight
386 to 0.46 $\text{mm h}^{-1} \text{MPa}^{-1}$. This resulted in a narrower water potential gradient between root zone and sunlit
387 leaf and in a higher transpiration rate on 19 July.

388 [Insert Figure 10 here]

389 Seasonal average of different midday hydraulic conductance components (root system hydraulic
390 conductance - $K_{\text{soil_root}}$, stem hydraulic conductance - K_{stem} , and whole plant hydraulic conductance -
391 $K_{\text{soil_plant}}$) are shown in Figure 11. In the same year, the K_{stem} was not much different among F1P3, F2P2, and
392 F2P3 plots. The K_{stem} of those plots was slightly higher than in the F1P2 in both years. In general, the $K_{\text{soil_root}}$
393 was lower than the K_{stem} . Overall, the estimated $K_{\text{soil_plant}}$ was around $1 / (1/K_{\text{soil_root}} + 1/K_{\text{stem}})$ regardless of
394 soil types, years, and water treatments. The $K_{\text{soil_root}}$ and $K_{\text{soil_plant}}$ in the F1P2 in 2018 was much lower than

395 the remaining plots while the $K_{\text{soil_root}}$ and $K_{\text{soil_plant}}$ were not much different among plots in 2017. Our results
396 indicated that there was an impact of soil hydraulic conductance on $K_{\text{soil_root}}$ and $K_{\text{soil_plant}}$. Although there is
397 a large difference in total root length between the two soil types (e.g. F1P3 versus F2P2 or F2P3 versus
398 F2P2), $K_{\text{soil_root}}$ and $K_{\text{soil_plant}}$ in those two plots were not much different. This could be explained by the fact
399 that $K_{\text{soil_plant}}$ was not only depended on root length but also depended on the variability of root segment
400 hydraulic conductance.

401 [Insert Figure 11 here]

402 **3.3. Relative importance of root and leaf area growth to transpiration and crop performance at canopy** 403 **level**

404 Drought stress was observed in the rainfed plot (F2P2) in the second week of June 2017 with mild leaf
405 rolling. The crop then recovered due to sufficient rainfall and lower evaporative demand. Drought stress
406 occurring again at the stem elongation phase caused reduction of plant size (height and stem diameter)
407 (Supplementary material 4) as well as a slight reduction of leaf area and biomass in this plot
408 (Supplementary material 3a & 3c). Transpiration per unit of leaf area did not differ much among water
409 treatments and soil types in 2017 (Figure 12). The opposite was the case for the transpiration rate per unit
410 of root length. The observed root length at different soil depths (Figure 2) and total root length for two
411 plots in the stony soil was much smaller than in the silty soil (Figure 3). Therefore, transpiration per unit
412 of root length in the stony soils (F1P2 & F1P3) was almost 3 times higher than transpiration in the silty soil.
413 For the same soil, transpiration per unit root length of the irrigated treatment was slightly larger than in
414 the rainfed plot.

415 [Insert Figure 12 here]

416 The differences in sap flow per plant between water treatments and soil types were more pronounced in
417 2018 (Figure 13). The highest transpiration rate was observed in the irrigated plots (F1P3 & F2P3), followed

418 by the rainfed plot of the silty soil (F2P2) and it was lowest in the rainfed plot of the stony soil (F1P2).
419 These observations were in line with the differences in biomass and leaf area index between the
420 treatments (Supplementary material 3b & 3d) and plant size (Supplementary material 4b-c-d). In 2018,
421 severe leaf rolling was observed in the rainfed plot (F1P2) from the beginning of June until the end of the
422 growing period in 2018 (Supplementary material 3d). Similar to 2017, transpiration per unit of root length
423 was much higher in the stony plots as compared to silty plots. Also, for the silty soil, transpiration per unit
424 of root length of the irrigated plot (F2P3) was higher than in the rainfed plot (F2P2).

425 [Insert Figure 13 here]

426 Higher cumulative transpiration in the irrigated plots did not result in higher transpiration use efficiency
427 (TUE) in both soil types (Figure 14). For instance, TUE were 16.87 g mm^{-1} and 15.59 g mm^{-1} for F1P2 and
428 F2P2, respectively, while they were 15.47 and 14.79 g mm^{-1} for F1P3 and F2P3, respectively, in 2017 (Figure
429 14A). For the same soil, the rainfed plot showed slightly higher TUE than the irrigated plot. When
430 comparing the TUE of maize of the two soil types for the same water treatment, TUE at the stony soil was
431 almost the same in silty soil. The TUE was not much different among treatments and soil types in 2018.
432 Overall, TUE in 2017 was higher as compared to 2018 (Fig. 14b).

433 [Insert Figure 14 here]

434 **4. Discussions**

435 **4.1. Effects of soil types, water application, and climatic condition on root growth**

436 Our root observations showed that soil type considerably affected root growth more than water treatment
437 (Figure 2). Root growth was strongly inhibited by the stony soil where much lower root length was
438 observed than in the silty soil, especially in the deeper soil layers. This was consistent with the findings
439 reported in (Morandage et al., 2021) where a linear increase of stone content resulted in a linear decrease
440 of rooting depth across all stone contents and developmental stages. Also, both simulations and

441 observations indicated that rooting depth was increased due to the presence of cracks in the lower
442 minirhizontron facility (Morandage et al., 2021) which could explain the high root length between 40 and
443 120 cm soil depths which was observed in the silty soil in both years.

444 In terms of the ratios of root length to shoot biomass, Ordóñez et al., (2020) has reported much larger
445 figures of for instance 880 cm g^{-1} in different locations and under different N application rates in maize
446 growing in the Midwest of US. Jorda et al., (2022) reported a wide range of ratios of root length to shoot
447 biomass from 200 to 1000 cm g^{-1} around flowering time of maize depending on the wild type and root hair
448 mutant genotypes growing on either loamy or sandy soils. More roots and higher ratios of root length to
449 shoot biomass were found in the sand than in the loam in both wild type and root hair mutant genotypes
450 (Jorda et al., 2022; Vetterlein et al., 2022). Cai et al., (2018) observed much larger ratios of root length to
451 shoot biomass in drought stressed plots than in irrigated plot in both soil types in winter wheat which
452 indicated the alternation of sink: source relationships to cope with water stress. This study emphasized
453 that more assimilates are used to promote root growth and extract more water under drought stress.
454 However, this was not the case for the stony soil in our work where the drought stress was more
455 pronounced, especially in 2018. A drop of soil water potential (Supplementary material 2b), thus effective
456 soil water potential (Figure 8a) was substantial from 10th July 2018 toward the harvest in the rainfed plot
457 in the silty soil (F2P2) which was consistent with the reduction of leaf water potential (Fig. 8b), leaf area
458 (Supplementary material 3c), total dry matter (Supplementary material 3d), and crop height
459 (Supplementary material 4b) as compared the irrigated plot (F2P3). This indicates a mild water stress in
460 2018 in the rainfed plots on the silty soil. The larger ratios of root length to shoot biomass in this F2P2 plot
461 in 2018 as compared to F2P3 could be explained by the change of source: sink relations where more
462 assimilates were devoted to root growth, even at a later growth stage. Moreover, the low stone content
463 and soil cracks (Morandage et al., 2021) might favor root growth in the deeper soil layers which are close
464 to the shallow soil water table in the rhizotrone facility with silty soil (Vanderborgh et al., 2010). In

465 conclusion, both soil texture and water conditions influenced the root growth, however, effects of the
466 former on root length was more pronounced than the latter.”

467 **4.2. Effects of soil types, water application, and climatic condition on stomatal conductance,** 468 **photosynthesis, transpiration, leaf water potential, and plant hydraulic conductance**

469 **4.2.1. Leaf water potential and stomatal conductance as affected by soil water conditions**

470 In the previous work, Koehler et al., (2022) reported that maize stomata closed at lower negative leaf
471 water potentials in sand than in loam growing under controlled environment. Cai et al., (2022b)
472 investigated transpiration response of pot-grown maize in two contrasting soil textures (sand and loam)
473 and exposed to two consecutive VPD levels (1.8 and 2.8 kPa). Transpiration rate decreased at less negative
474 soil matric potential in sand than in loam at both VPD levels. In sand, high VPD generated a steeper drop
475 in stomatal conductance with decreasing leaf water potential which indicated that the transpiration and
476 stomatal responses depend on soil hydraulics. In our study, stomata closed earlier and at more negative
477 soil and leaf water potentials in the stony soil than in the silty soil (see Fig. 4, 5, 6 and 7). The lower soil
478 water holding capacity of the stony soil compared to the silty soil resulted in lower soil water potential
479 and smaller total plant hydraulic conductance which in turn led to earlier stomatal closure and to more
480 negative soil water potential in the stony soil.

481 Stomatal control is an early and effective response to water stress to prevent the plant from water loss
482 and dehydration. Maize is considered as an isohydric plant which closes its stomata to maintain leaf water
483 potential above critical levels (Tardieu and Simonneau, 1998). Our results showed that minimum leaf
484 water potential varied among treatments (-1.5 MPa for F1P3, F2P2, and F2P3 and up to -2 MPa for F1P2
485 in 2017, while in 2018 minimum values were -2 MPa for F2P3, F2P2, and F2P3 and -2.7 MPa for F1P2) (Fig.
486 7 and Fig. 8, Fig. 9). Large variability of minimum LWP has been reported for maize genotypes. Leaf water
487 potential can be limited at quite high values, for instance -0.8 MPa in some lines of maize, while values as

488 low as -1.5 MPa have also been recorded (Welcker et al., 2011). Some drought-tolerant maize genotypes
489 close stomata at less negative leaf water potential under soil water depletion than more sensitive ones,
490 which is associated with their ability to avoid xylem embolism and hydraulic failure (Cochard, 2002; Tyree
491 et al., 1986; Li et al., 2009). However, our results show that the leaf water potential threshold can vary
492 within the same genotype depending on soil types, climatic conditions and water management. It should
493 be noted the constant ψ_{leaf} level (around -1.8 MPa) under different soil water regimes reported in Tardieu
494 and Simonneau (1998) that was associated with high VPD values, was based on observations from a single
495 day. Measurements on ψ_{leaf} and Gs for different days during several growing seasons have been rarely
496 reported for maize. The results of our study confirmed that maize appears to maintain its ψ_{leaf} at around -
497 1.5 to -2 MPa which depended on evaporative demand and levels of soil moisture (Fig. 1, Fig. 7, Fig. 8, and
498 Fig. 9). This has been reported recently in Nguyen et al. (2022a). Our current study, which investigates the
499 drivers of the modifications of ψ_{leaf} during the growing season, also confirmed that such stomatal
500 regulation and the ψ_{leaf} were mediated by soil hydraulics. Cochard, (2002) reported that stomatal closure
501 is complete between -1.6 and -2 MPa. In our study, the observed ψ_{leaf} was below -2 MPa for several days.
502 Similar values were also reported by Li et al. (2002) for field-grown maize in semiarid conditions. In our
503 study, leaf water potential dropped below -2 MPa in the rainfed plots to levels much lower than those
504 observed in the irrigated plots in 2018. This could imply different degrees of isohydry in maize. A
505 continuum exists in the degree to which stomata regulate the ψ_{leaf} for trees (Domec and Johnson, 2012;
506 Klein, 2014) or in grape-vine (Schultz, 2003). Also, cultivars of grape vine show large differences in
507 minimum ψ_{leaf} indicating differing degrees of isohydric behavior (Coupel-Ledru et al., 2014). When
508 comparing different herbaceous species, Turner et al., (1984) showed that there was a range of isohydric
509 behavior among the species in terms of the response to increasing vapor pressure deficit (VPD) under
510 sufficient soil moisture. However, conclusions concerning contrasting minimum ψ_{leaf} between 2017 and
511 2018 should not be overemphasized. Observed extremely low ψ_{leaf} correspond with the extremely low Gs
512 and were further accompanied by complete leaf curling in rainfed treatment under stony soil in 2018 (Fig.

513 4, 5, and Fig. 9) due to the extremely dry and hot summer and severe soil dryness. In conclusion, our results
514 confirmed that the minimum ψ_{leaf} not only depended on genotypic differences but also was influenced by
515 soil types and soil hydraulic conductance.

516 **4.2.2. Hydraulic conductance components as affected by soil water conditions**

517 Estimates of hydraulic components in soil-plant-atmosphere continuum are important not only to
518 understand its underlying relationship to other crop characteristics (stomatal conductance, transpiration,
519 and photosynthesis) but also to provide modeling parameters in process-based soil-root-shoot models
520 (Nguyen et al., 2020; Sulis et al., 2019; Nguyen et al., 2022b). Measurement of the components of hydraulic
521 conductance are challenging under field conditions because it requires the estimation of transpiration and
522 root to leaf water potential gradients. To our knowledge, our results were unique with regard to the
523 dynamics of $K_{\text{soil_plant}}$ for field-grown maize on two soil types and under contrasting water, and climate
524 conditions. Our seasonal $K_{\text{soil_plant}}$ ranged from 0.12 mm h⁻¹ MPa⁻¹ to 0.9 mm h⁻¹ MPa⁻¹ (Fig. 8 & Fig. 9; Fig.
525 10, and Supplementary material 5). Root system hydraulic conductance ranged from 0.26 to 1.47 mm h⁻¹
526 MPa⁻¹ (Figure 11). Note that the unit of $K_{\text{soil_plant}}$ as mm h⁻¹ MPa⁻¹ could be equivalent to the unit of 10⁻⁵ h⁻¹
527 ¹ if one assumes 1MPa is approximately 10⁵ mm in terms of pressure head. Cai et al., (2018) reported root
528 hydraulic conductance in winter wheat from 0.05 to 0.5 mm h⁻¹ MPa⁻¹ in two similar soil types. Nguyen et
529 al., (2020) also reported $K_{\text{soil_plant}}$ in winter wheat from 0.0625 to 0.461 mm h⁻¹ MPa⁻¹. Meunier et al., (2018)
530 focused on estimating the root system hydraulic conductance of maize in a container experiment where
531 the range of $K_{\text{soil_plant}}$ was much larger from 0.37 to 36 mm h⁻¹ MPa⁻¹ for the plant density of 10 plant m⁻².
532 Jorda et al., (2022) estimated root system hydraulic conductance of 0.5 to 1.5 10⁻³ d⁻¹ which would be
533 roughly between 2 to 6 mm h⁻¹ MPa⁻¹. In our work, except the F2P2 in 2018, the stem hydraulic
534 conductance was 10% to 60% higher than root system hydraulic conductance. Gallardo et al., (1996)
535 reported that stem hydraulic conductance of wheat was lower than root system conductance at around
536 71 to 91 days after sowing (DAS), but they were similar at 102 DAS. In lupine, stem hydraulic conductance

537 was two times higher than root system conductance regardless of measured days. The larger root length
538 in wheat than lupine did not necessarily result in higher root conductance in wheat. Together with this
539 study, our study emphasizes the values of stem hydraulic conductance compared to the root hydraulic
540 conductance in maintaining water potential gradient from shaded leaf or plant color to the sunlit leaf.

541 Our results showed clear differences in $K_{\text{soil_plant}}$ among treatments where much lower $K_{\text{soil_plant}}$ was
542 observed in the F1P2 as compared to F2P2 (see Figure 10 for 2018; Figure 8 and 9 and Supplementary
543 material 5 for both years). This indicated the soil texture dependence for whole plant hydraulic
544 conductance. Maize plants with the shorter root system (i.e. rainfed plot in the stony soil in 2018) (Fig. 3)
545 had lower plant hydraulic conductance. Our results indicated that there was an impact of soil hydraulic
546 conditions on $K_{\text{soil_plant}}$ via the reduction of root system hydraulic conductance. Our analysis for three
547 consecutive measurement days in 2018 (Fig 10) showed that in the silty soil, $K_{\text{soil_plant}}$ decrease when soil
548 water potentials are becoming more negative. For instance, in the silty soil in 2018 when the soil water
549 potentials were considerably lower in the rainfed than in the irrigated plot (e.g. after 10th July), $K_{\text{soil_plant}}$
550 was lower in the rainfed than in the irrigated plot. In the stony soil, the $K_{\text{soil_plant}}$ and leaf water potentials
551 seems to decrease more considerably (compared to the silty soil) when the soil water potentials become
552 more negative. In other words, $K_{\text{soil_plant}}$ increased considerably when the soil water potentials in the stony
553 soil increased. Koehler et al., (2022) analyzed the maize plant responses to soil drying under controlled
554 climate conditions with three soil types (sand, sandy loam, and loam). This study confirmed the impact of
555 soil texture on plant response to soil drying in various relationships. In their work, the soil-plant
556 conductance decreased in both sand and loam but at less negative water potentials in the sand than in the
557 loam. Root system hydraulic conductance decreased at less negative bulk soil water potential in the coarse
558 soil than in the fine soil (Vanderborgh et al., 2023). In our work, $K_{\text{soil_plant}}$ increased slowly after irrigation
559 mainly for the severe water stress plot (see F1P2 on 19 July in Fig 9d and 10c). This implied that added soil
560 water by irrigation took some time for recovery the soil-root contact within the rhizosphere.

561 **4.2.3. Relationships of stomatal conductance, transpiration, photosynthesis with plant hydraulic**
562 **variables**

563 In 2017, our estimated midday effective soil water potential ($\psi_{\text{soil_effec MD}}$) did not vary much (between soil
564 types and treatments) which was consistent with the low variability in midday sunlit leaf water potential
565 ($\psi_{\text{sunlitleaf MD}}$) and $K_{\text{soil_plant}}$ among water treatments (Fig. 8). The $\psi_{\text{soil_effecMD}}$ was high (around -0.35 MPa)
566 while $\psi_{\text{sunlitleaf MD}}$ was around -1.5 MPa (Fig. 8c). In contrast, the difference of $\psi_{\text{soil_effec MD}}$, $\psi_{\text{sunlitleaf MD}}$, and
567 $K_{\text{soil_plant}}$ was higher among water treatments and soil types in 2018 as compared to 2017. Moreover, the
568 high VPD and air temperature in combination with the small precipitation in the main growing season in
569 2018 led to a stronger reduction of $\psi_{\text{soil_effec MD}}$ up to -0.75 MPa (i.e. in F1P2 in the stony soil on 17 and 18
570 July in 2018, Figure 9) and $\psi_{\text{sunlitleaf MD}}$ to -2.5 MPa. This low $\psi_{\text{soil_effec MD}}$ in F1P2 was associated with low
571 stomatal conductance (Fig. 9c), low $K_{\text{soil_plant}}$ (Fig. 9d), and strong transpiration reduction (Fig. 10a-b, Fig.
572 12, and Supplementary material 5). Our results were in line with the analysis from Cai et al., (2022a) which
573 revealed that water uptake depended on effective soil water potential which in turn depended on soil
574 water potential which differed between plots with different textures.

575 The transpiration rate and $K_{\text{soil_plant}}$ (slope of linear regression lines in Fig. 10a and b) were very low in the
576 rainfed plot under the stony soil (F1P2) which was associated with the large $\psi_{\text{difference}}$ (Fig. 10a & b) and the
577 lower stomatal conductance as compared to other plots (Fig. 9c). The $K_{\text{soil_plant}}$ slightly increased after
578 irrigation (18 July - DOY 199 in Fig. 10b) corresponding with the smaller $\psi_{\text{difference}}$ (Fig. 10b) and an increase
579 in stomatal conductance (Fig. 9c). Seasonal $K_{\text{soil_plant}}$ was low in the rainfed plot under stony soil (F1P2) with
580 the larger $\psi_{\text{difference}}$ (Supplementary material 5). In addition, our study showed that the midday stomatal
581 conductance, photosynthesis, and transpiration were significantly correlated only with midday $K_{\text{soil_plant}}$ in
582 the rainfed plot on the stony soil (F1P2) in 2018 where high VPD and temperature occurred
583 (Supplementary material 6, 7, and Supplementary material 8). Maize plants had lower plant hydraulic
584 conductance and more negative soil water potential in the rainfed plot in stony soil that and they exhibited

585 earlier stomatal closure as compared to the same plot in the silty soil. This was in line with a study from
586 Abdalla et al., (2022) which suggested that during soil drying, stomatal regulation of tomato is controlled
587 by root and soil hydraulic conductance. Recent work from Müllers et al., (2022) on faba bean and maize
588 suggested that differences in the stomatal sensitivity among plant species can be partly explained by the
589 sensitivity of soil-plant hydraulic conductance to soil drying. The loss of conductance has immediate
590 consequences for leaf water potential and the associated stomatal regulation. Cai et al., (2022b) also
591 showed that the decrease in sunlit leaf stomatal conductance was well correlated with the drop in soil-
592 plant hydraulic conductance, which was significantly affected by soil texture. This was confirmed in our
593 work where the stony soil strongly impacted on root growth, modulated $K_{\text{soil_plant}}$, and consequently
594 influenced the leaf stomatal conductance, photosynthesis, and transpiration.

595 **4.3. Relative contribution of water control by leaves and roots on transpiration and transpiration use** 596 **efficiency**

597 Responses of crops via stomatal control to reduce water loss at leaf scale while maintaining leaf
598 photosynthesis and water use efficiency were reported earlier (Nguyen et al., 2022a; Vitale et al., 2007).
599 In addition to that, in the maize experiments in 2017 and 2018 leaf rolling was observed in both rainfed
600 plots on the stony and the silty soil in the second week of June 2017 and from the beginning of June until
601 the end of the growing period in 2018. This indicates another dehydration avoidance mechanism resulting
602 from morphological adjustments which is an effective mechanism for delaying senescence (Aparicio-Tejo
603 and Boyer, 1983; Richards et al., 2002). Stomatal closure resulted in more reduction of transpiration and
604 assimilation in the rainfed plots than irrigated plots with the same soil type (Fig. 5, Fig. 6, Fig. 7, and Fig.
605 13A). There was reduction of shoot biomass (also stem size and leaf size adjustments) in F1P2 as compared
606 to other plots. However, the TUE was not smaller in this plot than the remaining plots. These observations
607 confirm that plant size adjustments through reduction of height, leaf width and length are efficient
608 responses to reduce water loss at canopy scale in addition to stomatal control at the leaf level.

609 Relative contribution of leaf area to transpiration has been highlighted in wheat where reduction of tiller
610 number resulted in significantly (lower LAI, thus lower canopy transpiration (Cai et al., 2018; Trillo and
611 Fernández, 2005; Nguyen et al., 2022a). However, root system conductance per unit of leaf area and per
612 unit root mass were strongly reduced and eventually more than reduction of leaf area under water stress
613 (Trillo and Fernández, 2005). In our work, expressing the transpiration per unit of root length on the one
614 hand allowed to analyze the role of total root length to water uptake. However, on the other hand, the
615 lower total root length did not necessarily result in a lower root water uptake and vice versa. For instance,
616 the rainfed plot of the treatment F2P2 had the larger total root length which could postpone the effect of
617 soil water limitations in drying soils due to greater ability to extract water from subsoils. Therefore,
618 transpiration was very similar between F2P2 and F2P3. Despite of the much lower total root length in the
619 stony soil, $K_{\text{soil_plant}}$ in the irrigated plot (F1P3) was not much lower than in the same water treatment in
620 the silty soil (F2P3, Fig. 8c, 9c, Fig. 10, and Supplementary material 5). This could be explained by the fact
621 that the $K_{\text{soil_plant}}$ variability was not only depended on root architecture (here the root length and
622 distribution) but also depended on the variability of root segment hydraulic properties which has also been
623 illustrated and discussed in Zwieniecki et al. (2002), Frensch and Steudle (1989), Meunier et al. (2018),
624 Couvreur et al. (2014), and Ahmed et al. (2018). Meunier et al. (2020) showed that more than 65% of the
625 variability of root system conductance of maize plants could be attributed to variability in root
626 architecture, which includes root length, whereas only 25% of the variability was attributed to root
627 segment hydraulic properties. However, the analysis of Meunier et al., (2020) neither included the impact
628 of root hairs nor the impact of rhizosphere conductivity but only focused on the root system hydraulic
629 conductance. Moreover, the contribution of shoot hydraulic conductance could be large in plants (Gallardo
630 et al., 1996; Trillo and Fernández, 2005; Sunita et al., 2014) which also confirmed in our work. In our work,
631 $K_{\text{soil_plant}}$ comprised root and shoot conductance which are directly influenced by soil hydraulics. Our
632 estimates of $K_{\text{soil_plant}}$ varied with transpiration and gradients of $\psi_{\text{sun\textit{lit}leaf}}$ and $\psi_{\text{soil_effec}}$. Thus, any change of
633 soil hydraulic conductance will change the root to shoot water potential. Consequently, it will affect the

634 gradients between shoot and root rhizosphere (Carminati and Javaux, 2020). Thus, our study is revealing
635 the importance of both soil texture characteristics and root phenotypic traits (here root length) in
636 regulating plant transpiration (Cai et al., 2022a). Other traits like root hair density (Cai et al., 2022a) or
637 higher root length density (Vadez, 2014) could contribute to the soil to root water potential and root-zone
638 hydraulic conductance where dense root hairs are delaying soil water deficit in drying soils. However,
639 contrasting results have shown that root hairs did not have an effect on root water uptake (see Jorda et
640 al. 2022). The role of root hairs could not be analyzed in our work which was based on the root data from
641 minirhizotron images.

642 **5. Conclusion**

643 We presented plant hydraulic characteristics and crop growth from root to shoot of maize under field-
644 grown conditions with two soil types (silty and stony), each soil with two water regimes (irrigated and
645 rainfed) for two growing seasons (2017, 2018). Our results confirmed that root length and ratios of root
646 length to shoot biomass were modulated by soil types and water treatment but less by seasonal
647 evaporative demand. Increase ratio of root length to shoot biomass has been an important response of
648 maize that allows plants to extract more water under drought stress that occurred rather in the silty soil
649 but less in the stony soil due to the higher content of stony material. Despite of lower root length in the
650 stony irrigated plot, transpiration rate was not much lower than in the silty irrigated plot. This could be
651 related to another property of the root such as root segment conductance or other root traits (e.g. root
652 hair). Further investigation with extensive measurements of roots including axial and radial root
653 conductance at field scale will be required to better explain the observed results.

654 Another conclusion is that stomatal regulation maintains leaf water potential at certain thresholds which
655 depends on soil types, soil water availability, and seasonal atmospheric demand. The stomata conductance
656 was smaller and decreased at more negative leaf water potentials in stony soil than in silty soil. The leaf
657 water potentials are affected by the soil-plant hydraulic conductance. In addition to stomatal regulation,

658 leaf growth and plant size adjustments are important to regulate the transpiration and water use efficiency
659 in the same year.

660 The lowest soil-plant hydraulic conductance was observed in the stony soil with severe drought stress as
661 compared to silty soil while its variation depends also on the soil water variation (before and after
662 irrigation). Root system and soil-plant hydraulic conductance depended strongly on soil hydraulic
663 properties. In the stony soil, which has a considerably smaller water holding capacity than the silty soil,
664 root length was considerably smaller than in the silty soil. Nevertheless water uptake per unit root length
665 was much larger than in the fine soil. This also means that the hydraulic conductance per unit root length
666 must have been much larger in the stony soil than in the fine soil. Cai et al., (2018) observed a similar effect
667 for winter wheat but they found much smaller differences in the root length normalized root conductance.
668 The higher root length normalized root conductance means that the anatomy of the root tissues must
669 have been influenced by the soil texture and compensated the considerably smaller root length in the
670 stony soil. Looking at the effect of water treatments in the silt soil, the non-irrigated plot had more roots
671 than the irrigated one and both had more roots in the year with high VPD. But the soil-root conductance
672 was higher in the irrigated plot than in the rainfed plot. This means that in the irrigated plot, the soil-root
673 conductance per unit root length was higher than in the rainfed plot. This could either be due to wetter
674 soil conditions and higher soil conductance or it could be due to a larger conductance of the root tissues.
675 Especially in 2017 when the silty soil was wetter, the slightly larger soil-root conductance in the irrigated
676 plot is most likely the result of larger root tissue conductance in the irrigated plot. Thus, how root
677 architecture (here represented simply by the total root length) and root tissue conductivities 'respond' to
678 drought stress might be opposite depending on the comparisons that are made. When the stony soil and
679 silt soil are compared, the higher 'stress' due to lower water availability in the stony soil resulted in less
680 roots with a higher root tissue conductance in the soil with more stress. When comparing the rainfed with
681 the irrigated plot in the silty soil, the higher stress in the rainfed soil resulted in more roots with a lower

682 root tissue conductance in the treatment with more stress. This illustrates that the 'response' to stress can
683 be completely opposite depending on conditions or treatments that lead to the differences in stress that
684 are compared. Therefore, it cannot be the 'stress' alone that defines how a plant will react and adapt its
685 root system. Modelling the impact of stress and the feedback between drought stress and plant
686 development is likely controlled by other properties or parameters that change with changing soil water
687 availability and atmospheric water demand than the plant stress level. Results from this study show that
688 soil-crop models should focus not only on simulating stomatal regulations to capture the response to
689 drought stress, but also require adequate representations of leaf growth and adjustments.

690

691

692

693

694

695

696

697

698

699

700

701

702

703 **List of Tables**

704 Table 1. Crop phenology and management information for different treatments in 2017 and 2018.

	2017				2018			
Soil types	Stony (F1)	Stony (F1)	Silty (F2)	Silty (F2)	Stony (F1)	Stony (F1)	Silty (F2)	Silty (F2)
Water treatments	Rainfed (P2)	Irrigated (P3)	Rainfed (P2)	Irrigated (P3)	Rainfed (P2)	Irrigated (P3)	Rainfed (P2)	Irrigated (P3)
Plot names	F1P2	F1P3	F2P2	F2P3	F1P2	F1P3	F2P2	F2P3
Growing season (days) [‡]	136	136	136	136	107	107	107	107
Cumulative rainfall (mm) [*]	248.7	248.7	248.7	248.7	91.3	91.3	91.3	91.3
Irrigation (mm)	0	130	0	130	66	257.6	0	257.6
Fertilizer application (mm/dd) (per hectare)	05/09:100 kg N + 40kg P ₂ O ₅ 07/06: 80 kg N + 40 kg K ₂ O				05/22: 100 kg N 05/30: 40 kg P ₂ O ₅ + 40 kg K ₂ O 06/27: 80 kg N			
Sowing date (mm/dd)	05/04				05/08			
Emergence date	05/09				05/13			
Tasseling date	07/09				07/09			
Silking date	07/14				07/11			
Harvest date	09/12				08/22			

705 Notes: [‡] from sowing to harvest; ^{*} for rainfall for whole growing season;

List of Figures

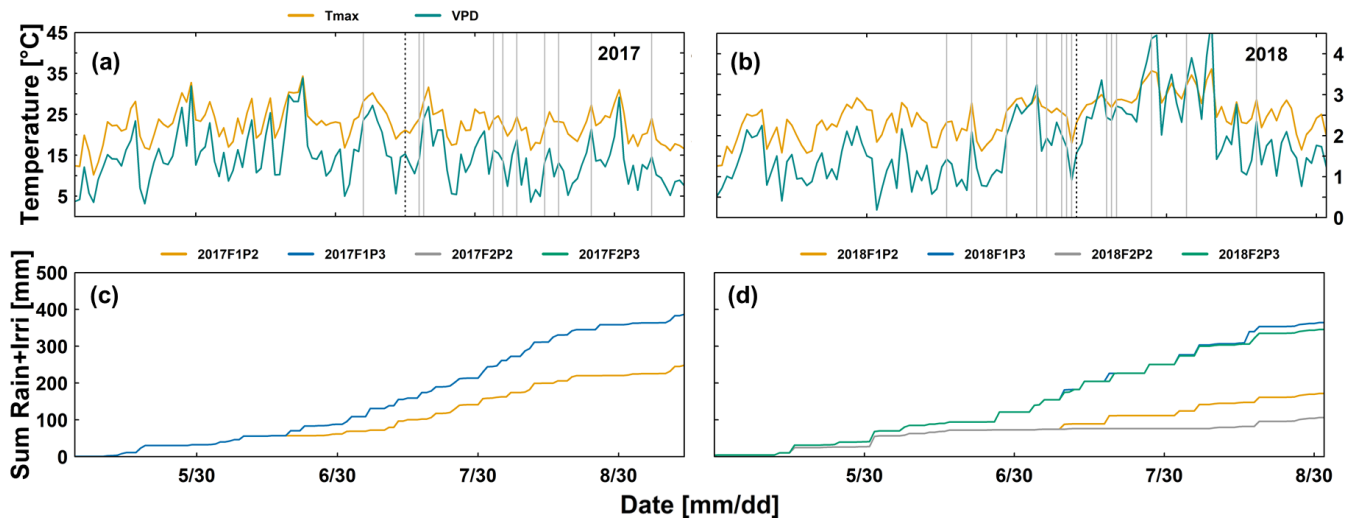


Figure 1: Daily maximum air temperature (Tmax) (°C), daily maximum air vapor pressure deficit (VPD) (kPa) in the two growing seasons (a) 2017 and (b) 2018 and cumulative (sum) of rainfall and irrigation from the rainfed (P2) and irrigated (P3) plots of the stony soil (F1) and silty soil (F2) in the two growing seasons (c) 2017 and (d) 2018. The black dashed vertical lines (a) and (b) indicate silking time. Grey vertical lines in (a) and (b) indicate the measured days for leaf gas exchange and leaf water potential. Two lines for 2017F2P2 and 2017F2P3 were overlapped by the lines from 2017F1P2 and 2017F1P3, respectively

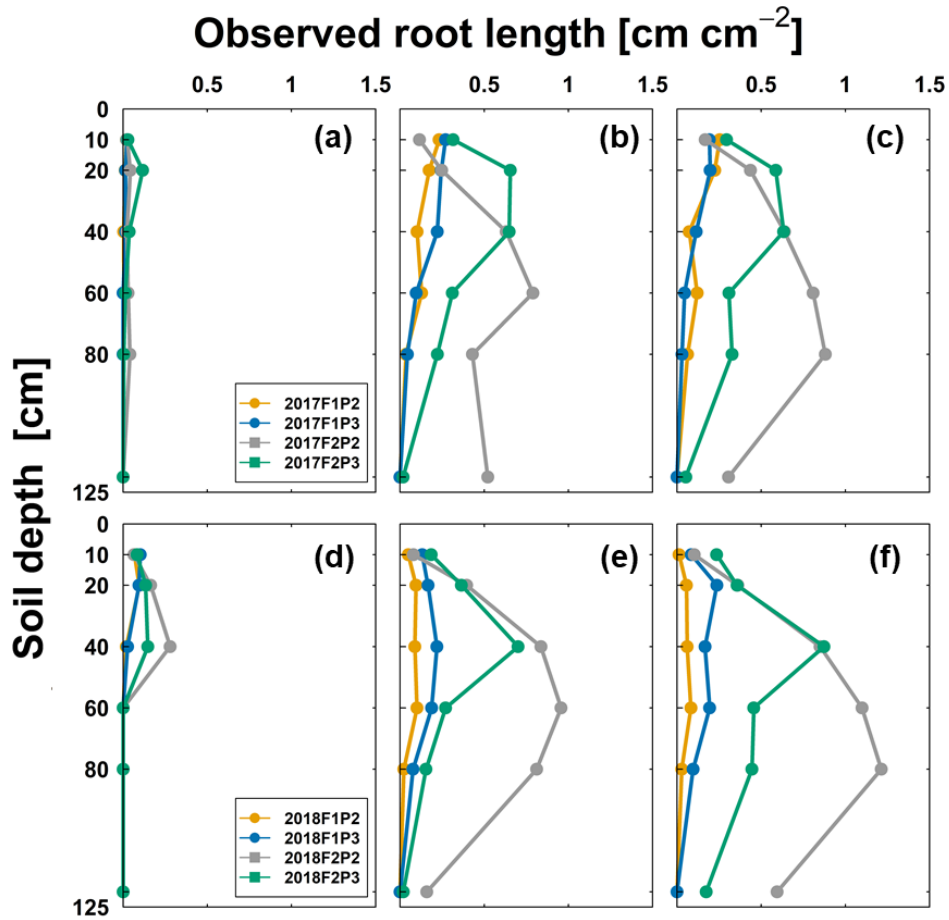


Figure 2: Observed root length from minirhizotubes (cm cm^{-2}) from 10, 20, 40, 60, 80, and 120 cm soil depth from the rainfed (P2) and irrigated (P3) plots of the stony soil (F1) and silty soil (F2) in the two growing seasons in 2017 (a - 8 June, b - at silking on 13 July, c - at harvest on 12 September) and in 2018 (d - 7 June, e - at one week after silking - 18 July, f - one week before harvest - 16 August).

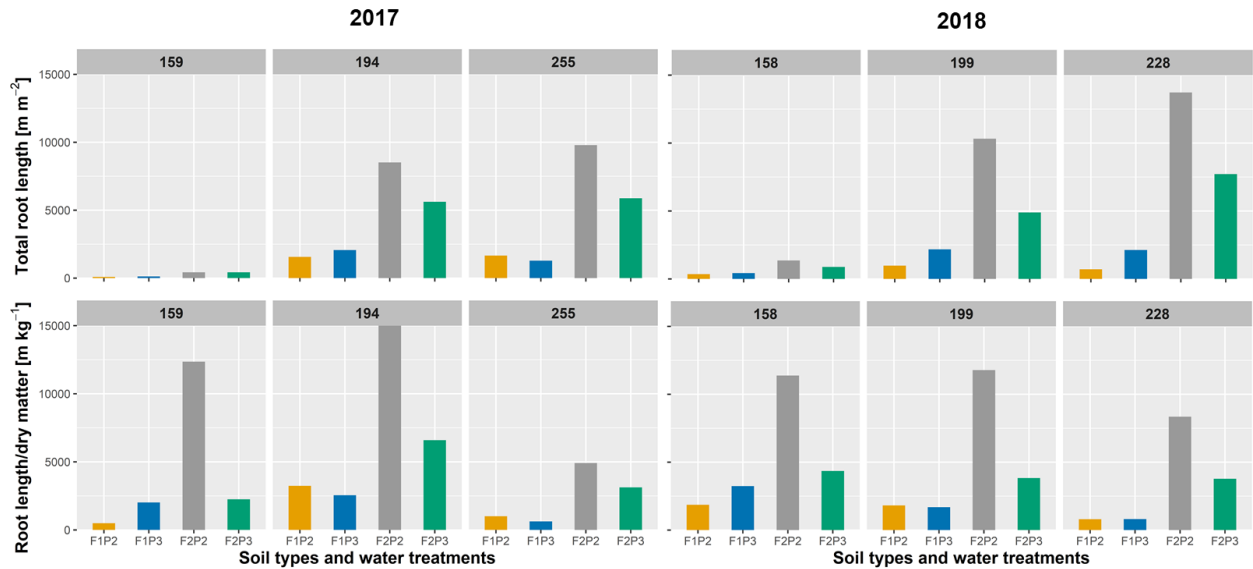


Figure 3: Observed root length from minirhizotubes (m m^{-2}) and ratio of root length per shoot dry matter (m kg^{-1}) from the rainfed (P2) and irrigated (P3) plots of the stony soil (F1) and silty soil (F2) in the two growing seasons (DOY 159, 194, and 255, left panel) in 2017 and in 2018 (DOY 158, 199, and 228, right panel) where on 8 June (DOY 159) at silking on 13 July (DOY194) 2017; and at harvest on 12 September (DOY 255) in 2017; 7 June (DOY 158), one week after silking on 18 July (DOY 199); and one week before harvest on 16 August (DOY 228) in 2018 (see also Figure 2).

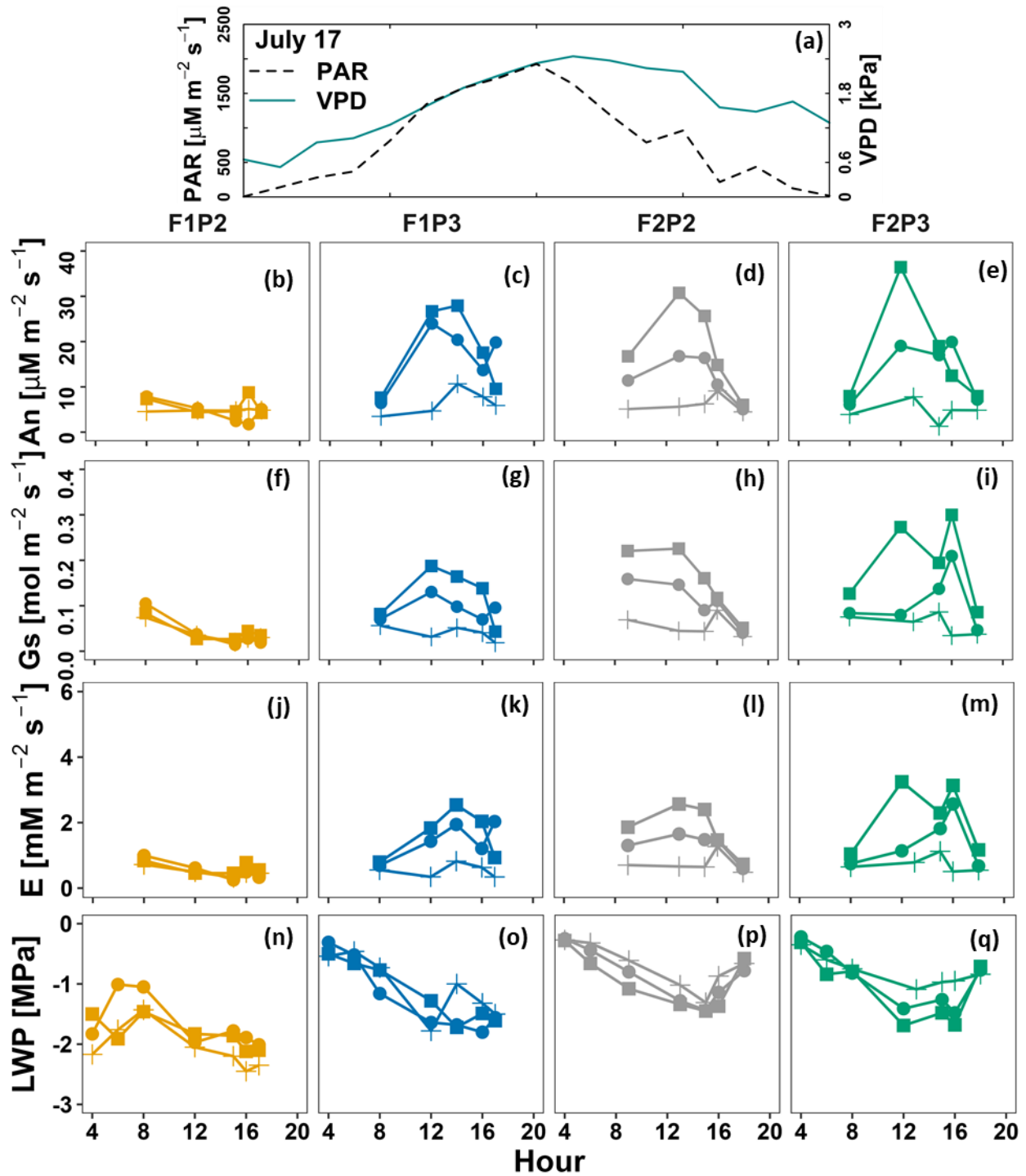


Figure 4. Diurnal course of (a) photosynthetically active radiation (PAR) and vapor pressure deficit (VPD), (b–e) leaf net photosynthesis (An), (f–i) leaf stomatal conductance (Gs), (j–m) leaf transpiration (E), and (n–q) leaf water potential (LWP) on 17 July in maize in 2018 before irrigation at the rainfed (P2) and irrigated (P3) plots of the stony soil (F1) and silty soil (F2). Measurement was carried out from shaded leaf (plus symbol with lines) and two sunlit leaves (solid dot - lines and solid square - lines).

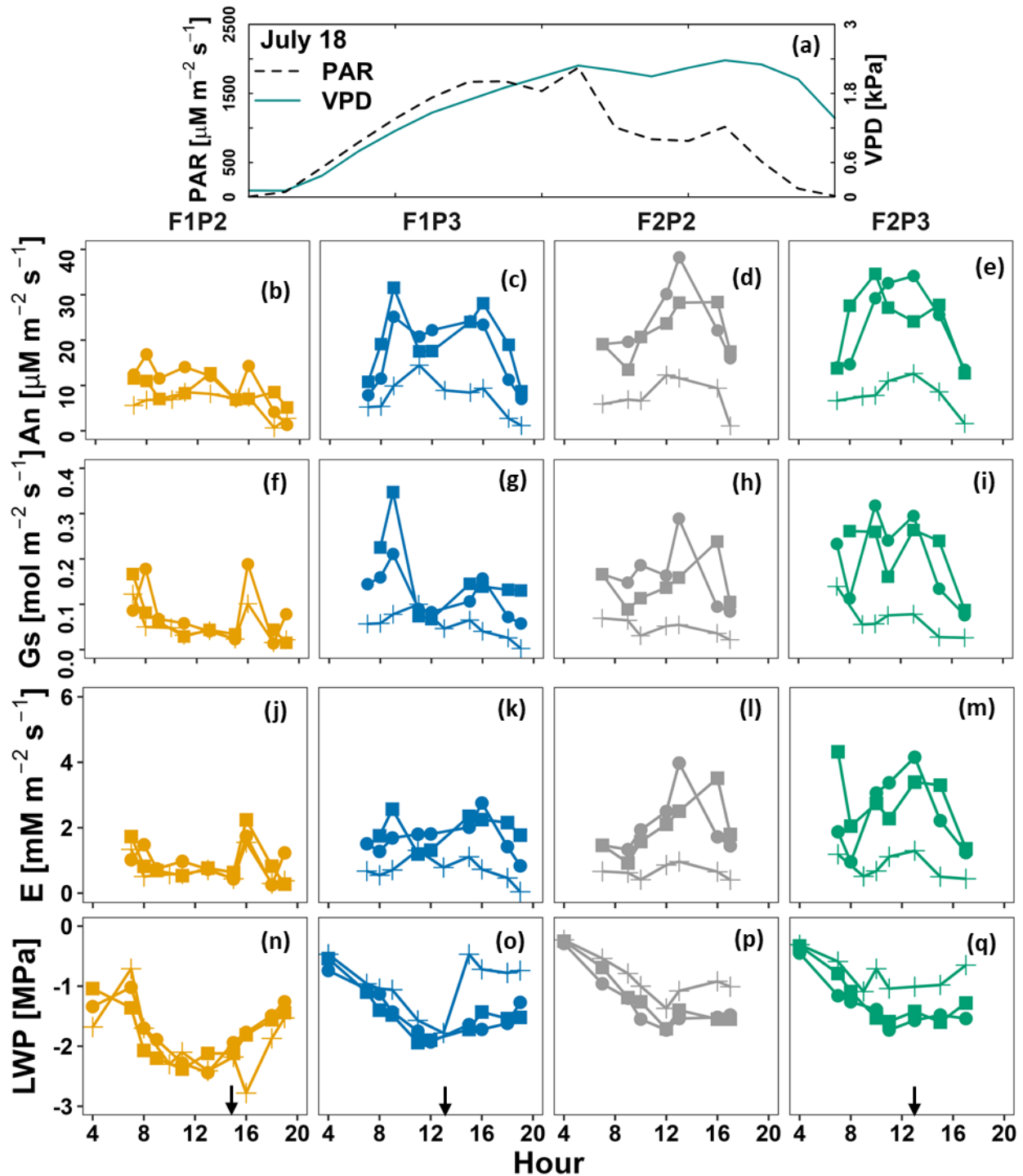


Figure 5. Diurnal course of (a) photosynthetically active radiation (PAR) and vapor pressure deficit (VPD), (b–e) leaf net photosynthesis (An), (f–i) leaf stomatal conductance (Gs), (j–m) leaf transpiration (E), and (n–q) leaf water potential (LWP) on 18 July in maize in 2018 before irrigation at the rainfed (P2) and irrigated (P3) plots of the stony soil (F1) and silty soil (F2). Measurement was carried out from shaded leaf (plus symbol with line) and two sunlit leaves (solid dot - lines and solid square - lines). Crop was irrigated at 1 PM, 1 PM, 4 PM for F1P3, F2P3, and F1P2, respectively (22.75 mm for each plot) (Supp. 2). Black arrows indicate time of irrigation.

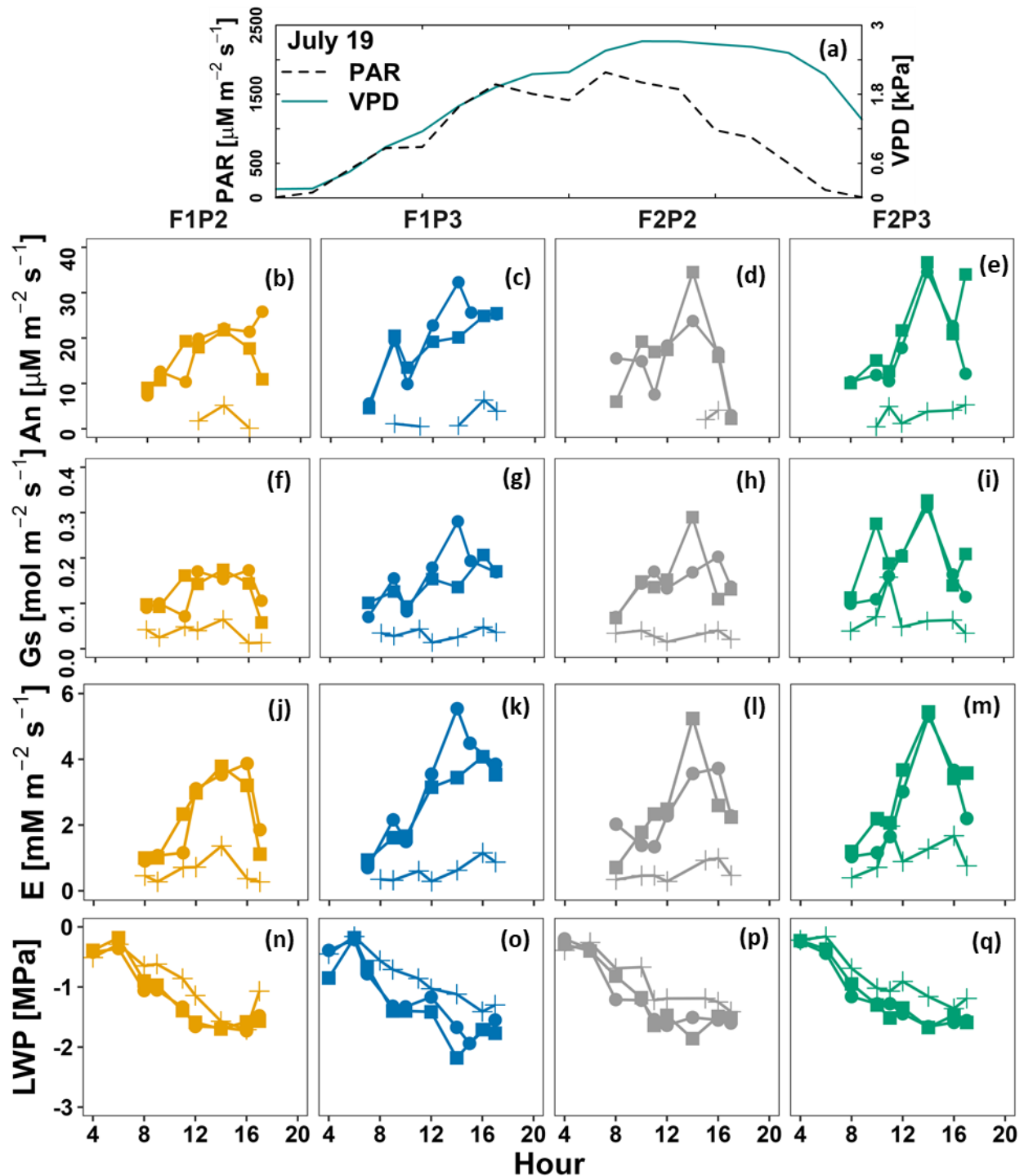


Figure 6. Diurnal course of (a) photosynthetically active radiation (PAR) and vapor pressure deficit (VPD), (b–e) leaf net photosynthesis (An), (f–i) leaf stomatal conductance (Gs), (j–m) leaf transpiration (E), and (n–q) leaf water potential (LWP) on 19 July in maize in 2018 after irrigation at the rainfed (P2) and irrigated (P3) plots of the stony soil (F1) and silty soil (F2). Measurement was carried out from shaded leaf (plus symbol with line) and two sunlit leaves (solid dot - lines and solid square -lines). Crop was irrigated on 18 July at 1 PM, 1 PM, 4 PM for F1P3, F2P3, and F1P2, respectively (22.75 mm for each plot) (Supp. 2).

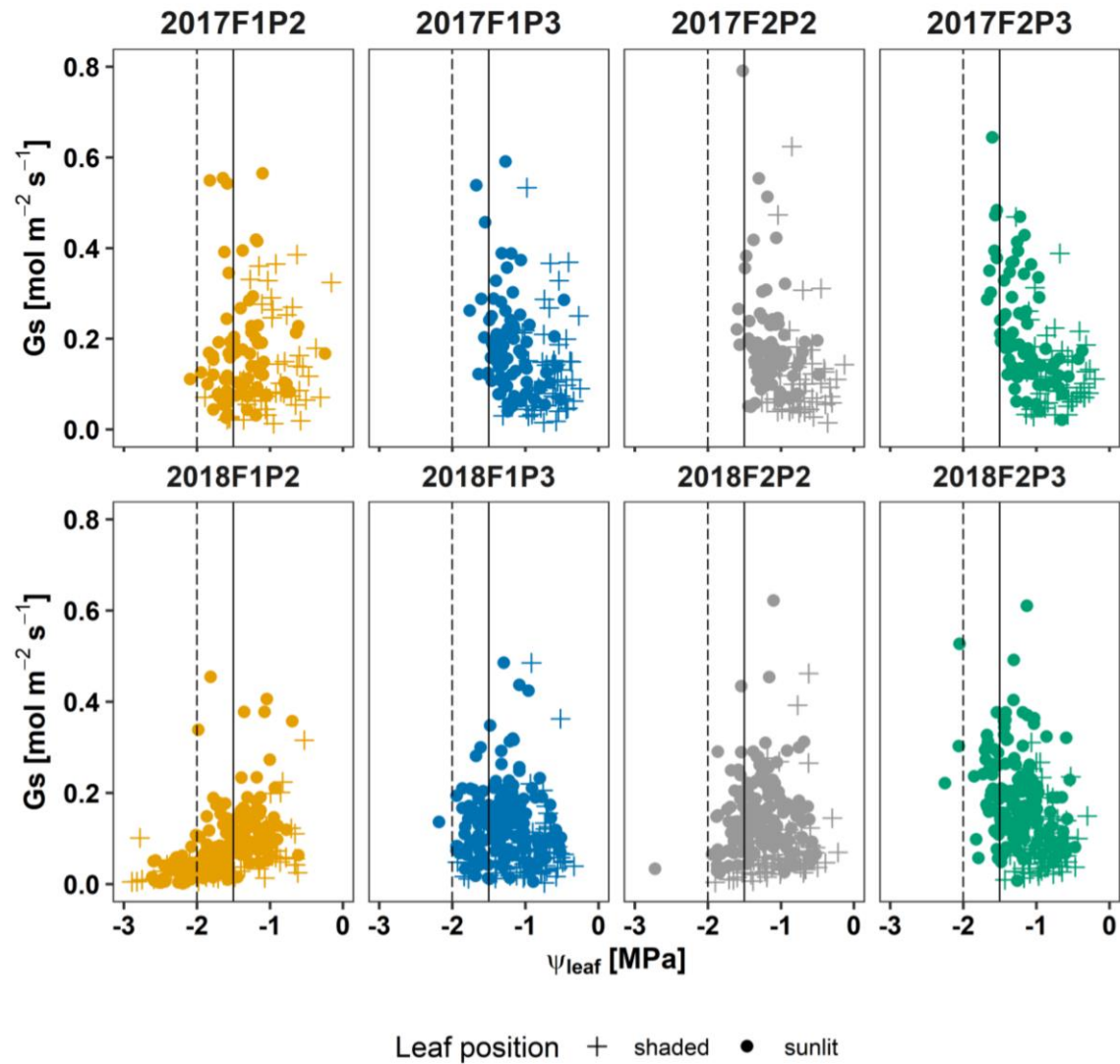


Figure 7: Seasonal stomatal conductance to water vapor (G_s) versus leaf water potential (ψ_{leaf}) in 2017 (top panel) and in 2018 (bottom panel) at the rainfed (P2) and irrigated (P3) plots of the stony soil (F1) and silty soil (F2). Vertically continuous and dashed lines indicated ψ_{leaf} at -1.5 and -2 MPa, respectively. Measurement was carried out from shaded leaf (plus symbol) and two sunlit leaves (solid dots)

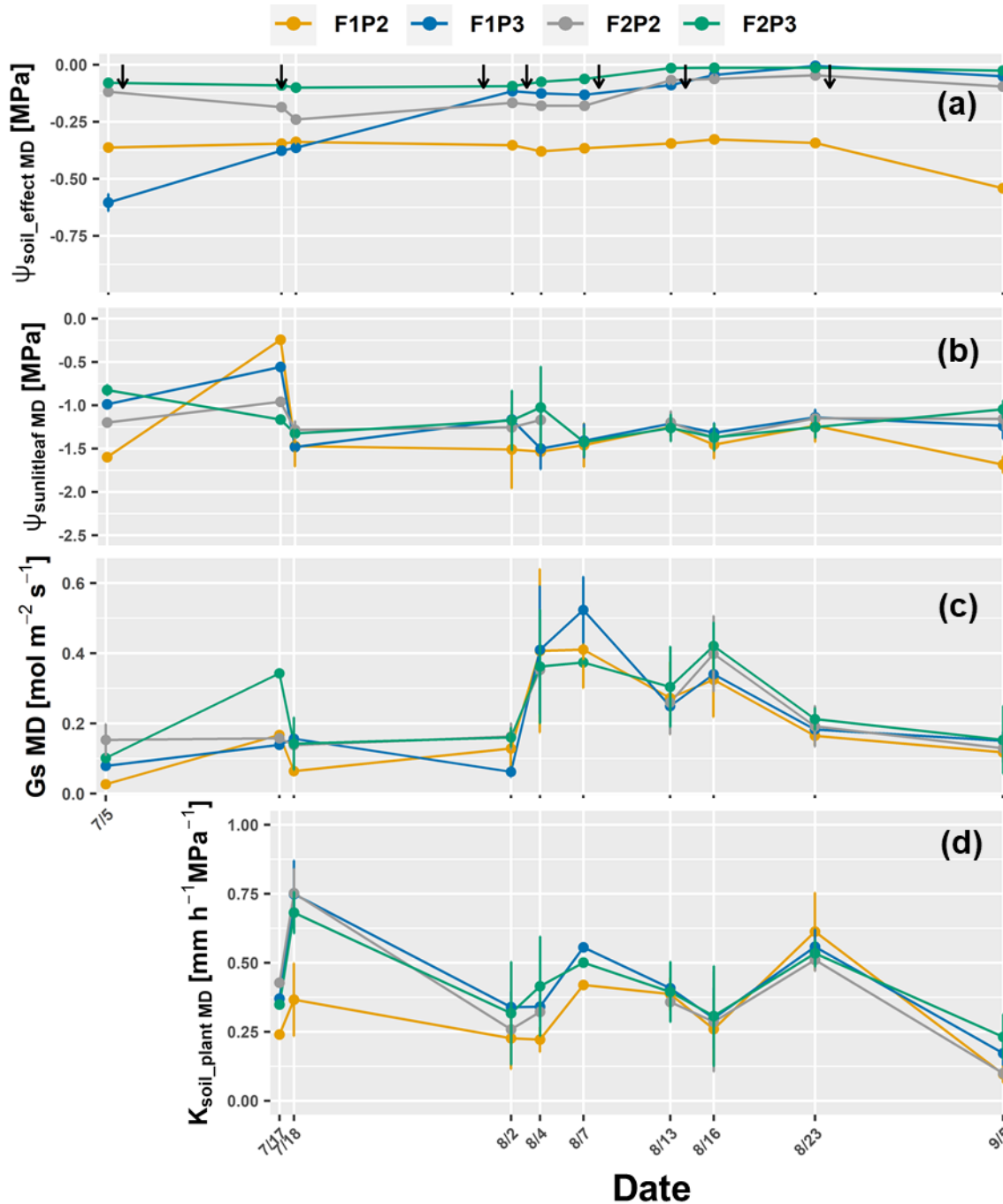


Figure 8: Dynamic of around midday (MD) of (a) the effective soil water potential ($\Psi_{\text{soil_effec, MD}}$) (b) sunlit leaf water potential ($\Psi_{\text{sunlitleaf MD}}$), (c) stomatal conductance (Gs MD) and (d) whole soil-plant hydraulic conductance ($K_{\text{soil_plant MD}}$) in the growing season 2017 from the rainfed (P2) and irrigated (P3) plots of the stony soil (F1) and silty soil (F2). Error bars indicate the standard deviation of the different values taken around midday (11 AM, 12AM, 1PM, and 2 PM) of different sunlit leaves. Whole soil-plant hydraulic conductance was shown from 17 July when sap flow was measured. The black arrows indicates the irrigation events for the irrigated treatments F1P3 and F2P3 in the showing period.

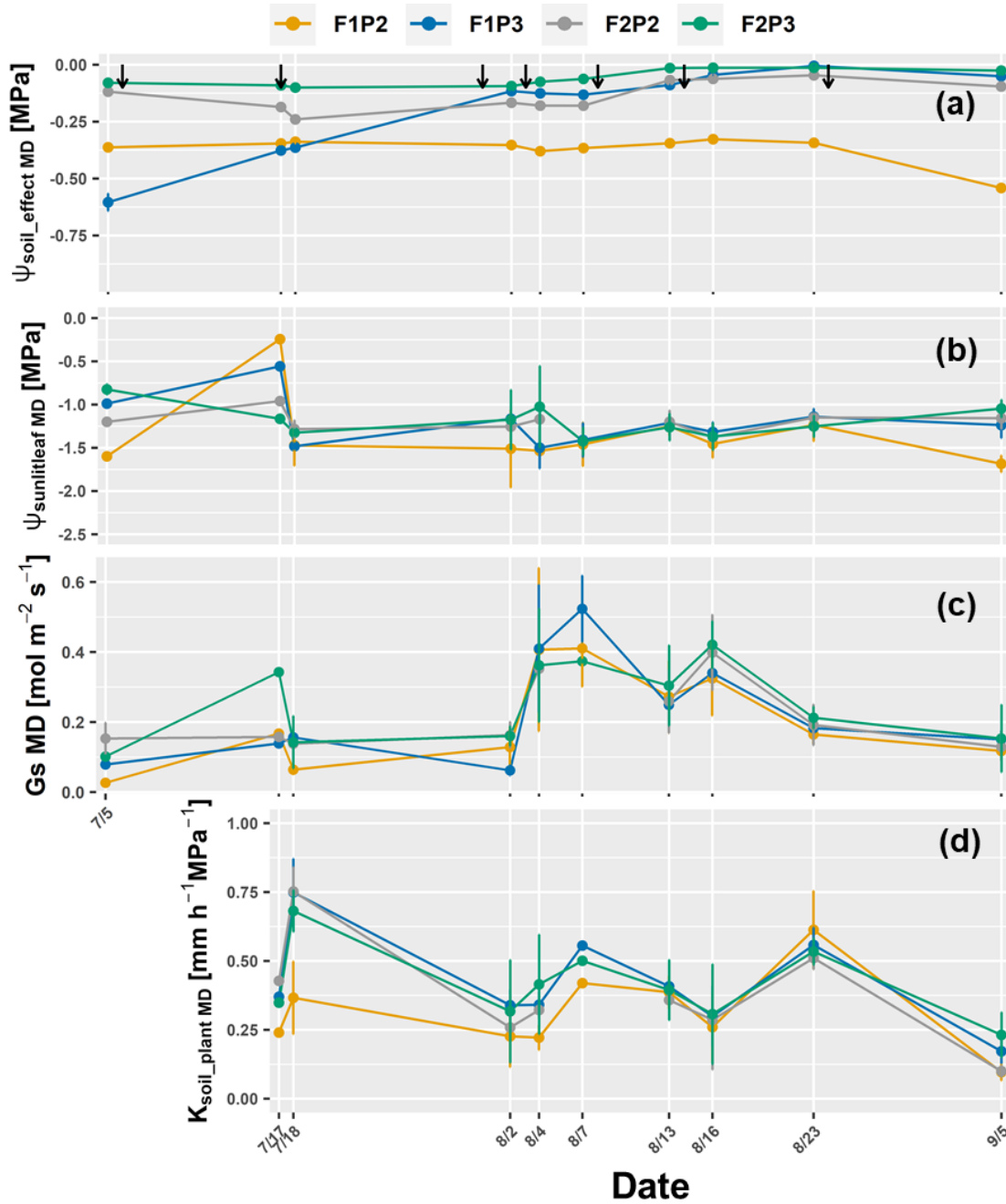


Figure 9: Dynamic of around midday (MD) of (a) the effective soil water potential ($\psi_{\text{soil_effec MD}}$) (b) sunlit leaf water potential ($\psi_{\text{sunlitleaf MD}}$), (c) stomatal conductance ($G_s \text{ MD}$) and (d) whole soil-plant hydraulic conductance ($K_{\text{soil_plant MD}}$) in the growing season 2018 from the rainfed (P2) and irrigated (P3) plots of the stony soil (F1) and silty soil (F2). Error bars indicate the standard deviation of the different values taken around midday (11 AM, 12AM, 1PM, and 2 PM) Leaf water potential and stomatal conductance were 2 sunlit leaves and one shaded leaf at each measured hour. Whole soil-plant hydraulic conductance was shown from 3 July when sap flow was measured. The black arrows indicates the irrigation events for the irrigated treatments F1P3 and F2P3 while the orange arrow indicates the irrigation application for the rainfed plot at the stony soil (F1P2).

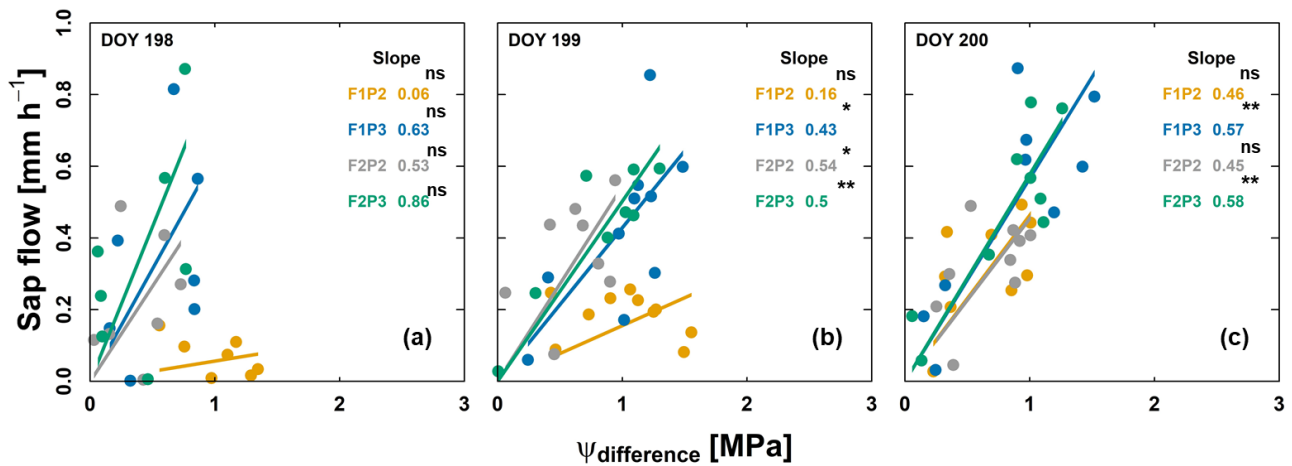


Figure 10: Relationship of sap flow and difference of effective soil water potential and sunlit leaf water potential ($\Psi_{\text{difference}}$) from the rainfed (P2) and irrigated (P3) plots of the stony soil (F1) and silty soil (F2) on three consecutive measurement days from predawn in 2018 (a) 17 July - DOY 198, (b) 18 July - DOY 199 and (c) 19 July - DOY 200. Crop was irrigated on 18 July (DOY 199) at 1 PM, 1 PM, and 4 PM for F1P3, F2P3, and F1P2, respectively (22.75 mm for each plot). The unit of slope in the linear regression (or soil-plant hydraulic conductance) is $\text{mm h}^{-1} \text{MPa}^{-1}$. Regression was based on the DEMING approach. The asterisk which are next to the slopes indicate a significant correlation between two variables according to Pearson method (ns: non-significant; * $p < 0.05$; ** $p < 0.01$; *** $p < 0.001$).

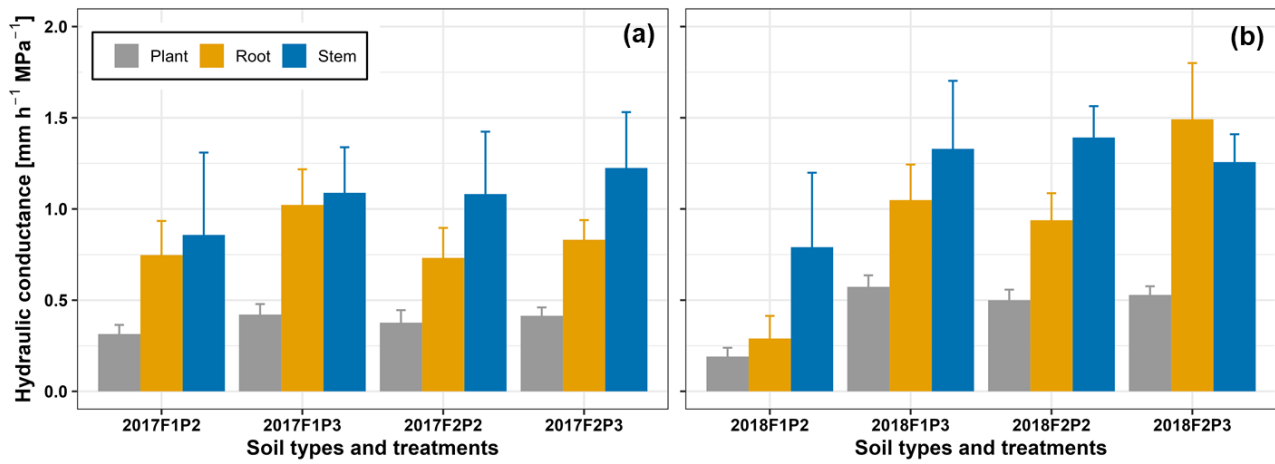


Figure 11: Comparison of different midday hydraulic components ($\text{mm h}^{-1} \text{MPa}^{-1}$): soil-plant (grey bars), soil-root (yellow bars), and stem (blue bars) from the rainfed (P2) and irrigated (P3) plots of the stony soil (F1) and silty soil (F2) in the two growing seasons (a) in 2017 and (b) in 2018. The error bars indicate the standard deviation from measurements around midday (11 AM, 12AM, 1PM, and 2 PM) in different measured days (in 2017 with $n = 4 \times 9$ days, Supplementary material 6, 7, and Fig. 8 and in 2018 with $n = 4 \times 10$ days, Supplementary material 6, 8, and Fig. 9).

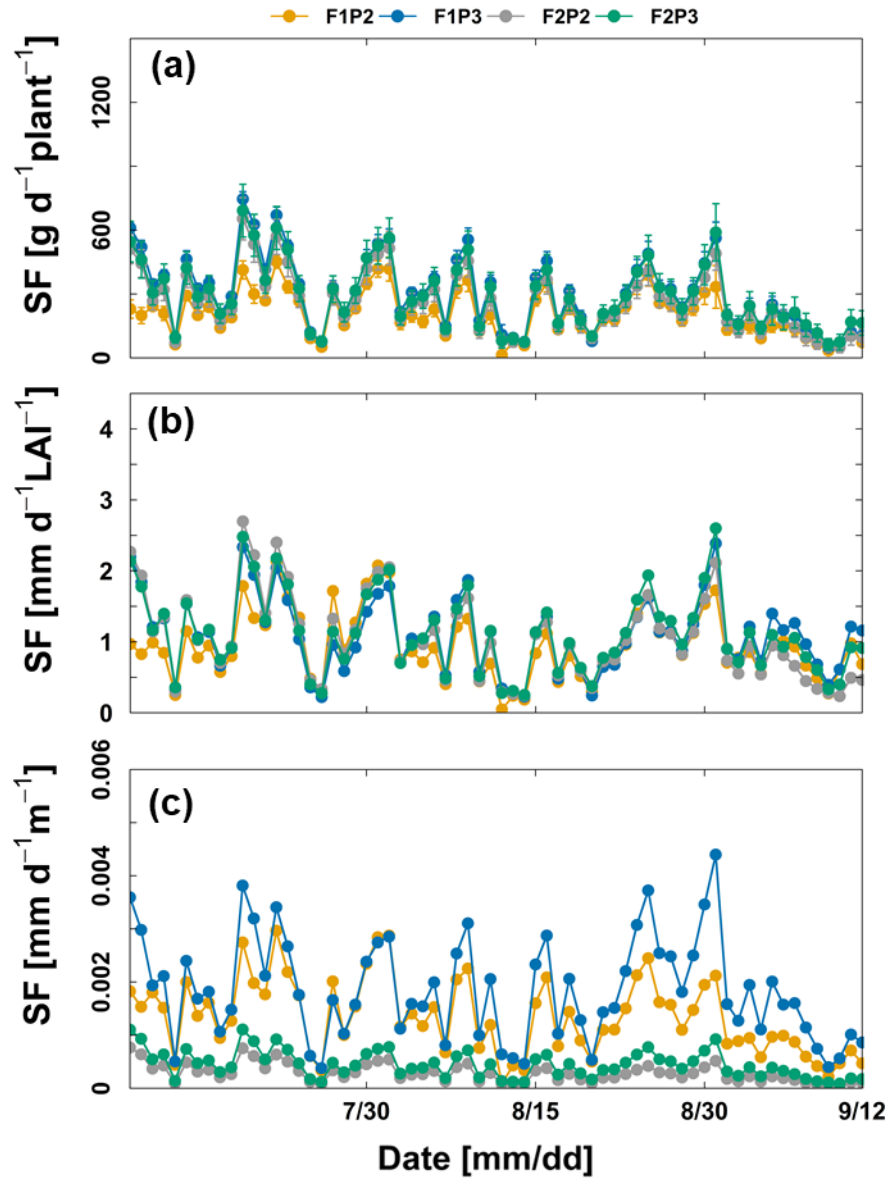


Figure 12: Comparison of sap flow (SF) in growing season 2017 from the rainfed (P2) and irrigated (P3) plots of the stony soil (F1) and silty soil (F2) with (a) sap flow per single plant (b) sap flow per leaf area index (LAI) and (c) sap flow per total root length. Data is shown from 9 July to 12 September 2017. Error bars in (a) indicate the standard deviation of the sap flow measurements in the five different maize plants.

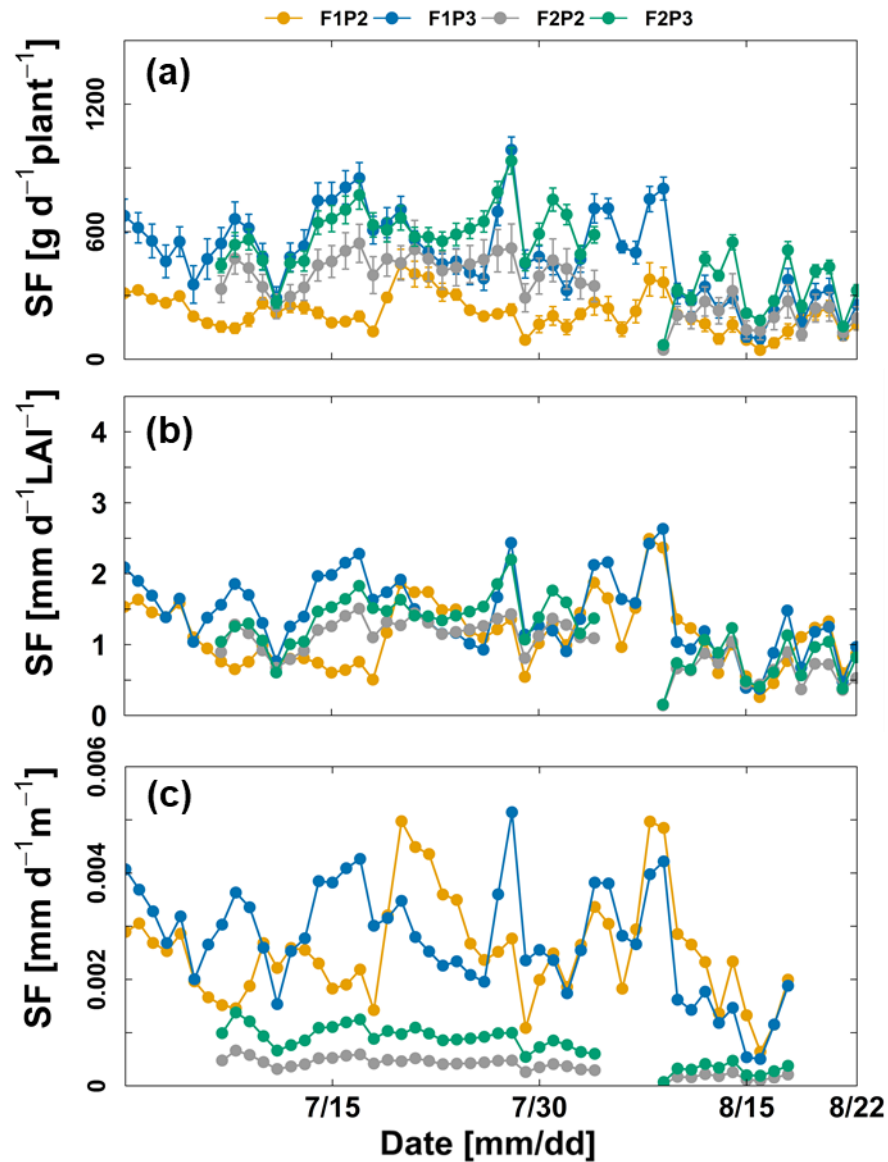


Figure 13: Comparison of sap flow (SF) in growing season 2018 from the rainfed (P2) and irrigated (P3) plots of the stony soil (F1) and silty soil (F2) with (a) sap flow per single plant (b) sap flow per leaf area index (LAI) and (c) sap flow per total root length. Data is shown in (a, b) from 29 June and 6 July for the stony soil (F1) and silty soil (F2), respectively to 21 August, 2018. Missing values of the beginning of the growing season and from 3 August to 6 August 2018 in the F2P2 and F2P3 were due to the missing values of measured sap flow because of sensor disconnection. Missing values in (c) at the end of the growing season in F2P2 and F2P3 was due to no availability of root measurement. Error bars in (a) indicate the standard deviation of the sap flow measurements in the five different maize plants.

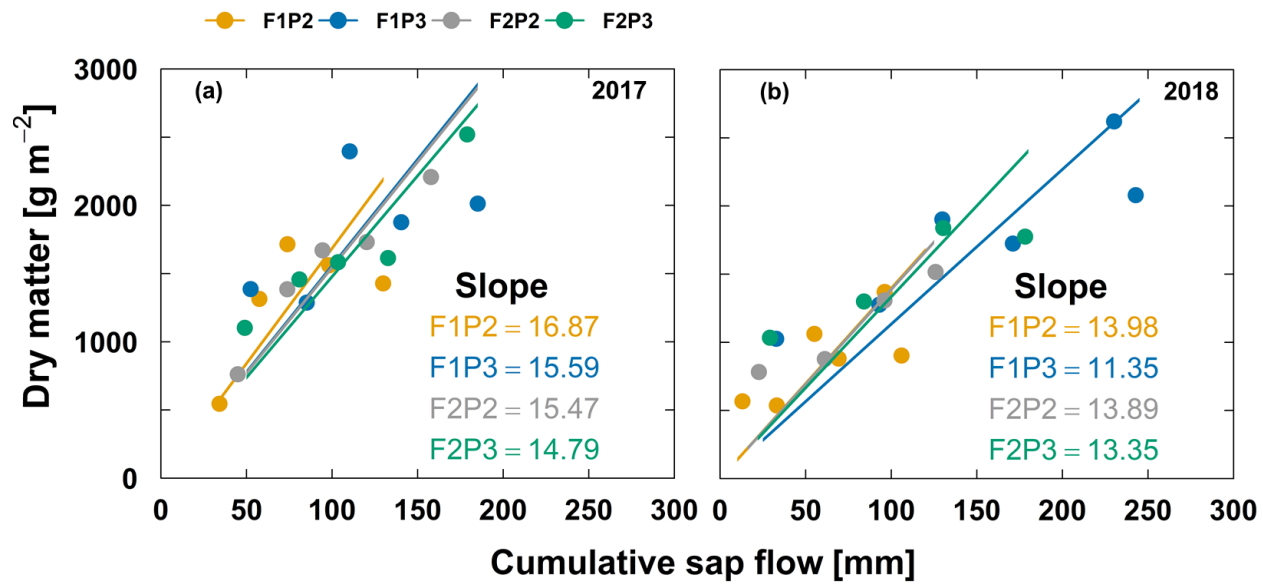


Figure 14: Relationship of aboveground dry matter and cumulative sap flow from the rainfed (P2) and irrigated (P3) plots of the stony soil (F1) and silty soil (F2) in the two growing seasons (a) 2017 and (b) 2018. The unit of slope linear relationship is g mm⁻¹. The less number of data points in (b) in 2018 from the F2P2 and F2P3 plots were due to the missing values of measured sap flow because of sensor disconnection. For aboveground dry matter, each point represents the average of two sampling replicates, except the harvest with 5 sampling replicates.

Acknowledgements

This work has partially been funded by Federal Ministry of Education and Research (BMBF) through European SUSCAP project – 031B0170B and COINS project and the Deutsche Forschungsgemeinschaft (DFG, German Research Foundation) under Germany’s Excellence Strategy – EXC 2070 – 390732324”. We acknowledge the support by the SFB/TR32 “Pattern in Soil–Vegetation–Atmosphere Systems: Monitoring, Modelling, and Data Assimilation” funded by the Deutsche Forschungsgemeinschaft (DFG). Thuy Nguyen and Thomas Gaiser also thank the DETECT – CRC 1502 research program which is funded by DFG. We thank Dr. Matthias Langensiepen for his supports and technical help in the TR32 project. We would like to thank all the student assistants and technicians for their considerable efforts to collect the data in the field and the laboratories.

Reference

- Abdalla, M., M.A. Ahmed, G. Cai, F. Wankmüller, N. Schwartz, et al. 2022. Stomatal closure during water deficit is controlled by below-ground hydraulics. *Ann. Bot.* 129(2): 161–170. doi: 10.1093/aob/mcab141.
- Abdalla, M., A. Carminati, G. Cai, M. Javaux, and M.A. Ahmed. 2021. Stomatal closure of tomato under drought is driven by an increase in soil-root hydraulic resistance. *Plant. Cell Environ.* 44(2): 425–431. doi: 10.1111/pce.13939.
- Ahmed, M.A., M. Zarebanadkouki, F. Meunier, M. Javaux, A. Kaestner, et al. 2018. Root type matters: Measurement of water uptake by seminal, crown, and lateral roots in maize. *J. Exp. Bot.* 69(5): 1199–1206. doi: 10.1093/jxb/erx439.
- Aparicio-Tejo, P., and J.S. Boyer. 1983. Significance of Accelerated Leaf Senescence at Low Water Potentials for Water Loss and Grain Yield in Maize1. *Crop Sci.* 23(6): crops1983.0011183X002300060040x. doi: <https://doi.org/10.2135/cropsci1983.0011183X002300060040x>.
- Bauer, F.M., L. Lärm, S. Morandage, G. Lobet, J. Vanderborght, et al. 2021. Combining deep learning and automated feature extraction to analyze minirhizotron images: development and validation of a new pipeline. *bioRxiv* (1): 2021.12.01.470811. <https://www.biorxiv.org/content/10.1101/2021.12.01.470811v1%0Ahttps://www.biorxiv.org/content/10.1101/2021.12.01.470811v1.abstract>.
- Bornemann*, L., M. Herbst, G. Welp, H. Vereecken, and W. Amelung. 2011. Rock Fragments Control Size and Saturation of Organic Carbon Pools in Agricultural Topsoil. *Soil Sci. Soc. Am. J.* 75(5): 1898. doi: 10.2136/sssaj2010.0454.
- Bourbia, I., C. Pritzkow, and T.J. Brodribb. 2021. Herb and conifer roots show similar high sensitivity to

- water deficit. *Plant Physiol.* 186(4): 1908–1918. doi: 10.1093/plphys/kiab207.
- Cai, G., M.A. Ahmed, M. Abdalla, and A. Carminati. 2022a. Root hydraulic phenotypes impacting water uptake in drying soils. *Plant Cell Environ.* 45(3): 650–663. doi: 10.1111/pce.14259.
- Cai, G., M. König, A. Carminati, M. Abdalla, M. Javaux, et al. 2022b. Transpiration response to soil drying and vapor pressure deficit is soil texture specific. *Plant Soil* (0123456789). doi: 10.1007/s11104-022-05818-2.
- Cai, G., J. Vanderborght, V. Couvreur, C.M. Mboh, and H. Vereecken. 2017a. Parameterization of Root Water Uptake Models Considering Dynamic Root Distributions and Water Uptake Compensation. *Vadose Zo. J.* 0(0): 0. doi: 10.2136/vzj2016.12.0125.
- Cai, G., J. Vanderborght, A. Klotzsche, J. van der Kruk, J. Neumann, et al. 2016. Construction of Minirhizotron Facilities for Investigating Root Zone Processes. *Vadose Zo. J.* 15(9): 0. doi: 10.2136/vzj2016.05.0043.
- Cai, G., J. Vanderborght, M. Langensiepen, A. Schnepf, H. Hüging, et al. 2018. Root growth, water uptake, and sap flow of winter wheat in response to different soil water conditions. *Hydrol. Earth Syst. Sci.* 22(4): 2449–2470. doi: 10.5194/hess-22-2449-2018.
- Cai, Q., Y. Zhang, Z. Sun, J. Zheng, W. Bai, et al. 2017b. Morphological plasticity of root growth under mild water stress increases water use efficiency without reducing yield in maize. *Biogeosciences* 14(16): 3851–3858. doi: 10.5194/bg-14-3851-2017.
- Carminati, A., and M. Javaux. 2020. Soil Rather Than Xylem Vulnerability Controls Stomatal Response to Drought. *Trends Plant Sci.* 25(9): 868–880. doi: 10.1016/j.tplants.2020.04.003.
- Carminati, A., M. Zarebanadkouki, E. Kroener, M.A. Ahmed, and M. Holz. 2016. Biophysical rhizosphere processes affecting root water uptake. *Ann. Bot.* 118(4): 561–571. doi: 10.1093/aob/mcw113.
- Choudhary, S., and T.R. Sinclair. 2014. Hydraulic conductance differences among sorghum genotypes to explain variation in restricted transpiration rates. *Funct. Plant Biol.* 41(3): 270–275. doi: 10.1071/FP13246.
- Cochard, H. 2002. Xylem embolism and drought-induced stomatal closure in maize. *Planta* 215(3): 466–471. doi: 10.1007/s00425-002-0766-9.
- Comas, L.H., S.R. Becker, V.M. V. Cruz, P.F. Byrne, and D.A. Dierig. 2013. Root traits contributing to plant productivity under drought. *Front. Plant Sci.* 4(NOV): 1–16. doi: 10.3389/fpls.2013.00442.
- Coupel-Ledru, A., É. Lebon, A. Christophe, A. Doligez, L. Cabrera-Bosquet, et al. 2014. Genetic variation in a grapevine progeny (*Vitis vinifera* L. cvs GrenachexSyrah) reveals inconsistencies between maintenance of daytime leaf water potential and response of transpiration rate under drought. *J. Exp. Bot.* 65(21): 6205–6218. doi: 10.1093/jxb/eru228.
- Couvreur, V., J. Vanderborght, X. Draye, and M. Javaux. 2014. Dynamic aspects of soil water availability for isohydric plants: Focus on root hydraulic resistances. *water Resour. Res.* 50: 8891–8906. doi: 10.1002/2014WR015608. Received.
- Couvreur, V., J. Vanderborght, and M. Javaux. 2012. A simple three-dimensional macroscopic root water uptake model based on the hydraulic architecture approach. *Hydrol. Earth Syst. Sci.* 16: 2957–2971. doi: 10.5194/hess-16-2957-2012.
- Daryanto, S., L. Wang, and P. Jacinthe. 2016. Global Synthesis of Drought Effects on Maize and Wheat

- Production. PLoS One 11(5): 1–15. doi: 10.1371/journal.pone.0156362.
- Draye, X., Y. Kim, G. Lobet, and M. Javaux. 2010. Model-assisted integration of physiological and environmental constraints affecting the dynamic and spatial patterns of root water uptake from soils. *J. Exp. Bot.* 61(8): 2145–2155. doi: 10.1093/jxb/erq077.
- Domec, J., and D.M. Johnson. 2012. Does homeostasis or disturbance of homeostasis in minimum leaf water potential explain the isohydric versus anisohydric behavior of *Vitis vinifera* L. cultivars? *Tree* 32: 245–248. doi: 10.1093/treephys/tps013.
- Domec, J., and M.L. Pruyn. 2008. Bole girdling affects metabolic properties and root, trunk and branch hydraulics of young ponderosa pine trees. *Tree Physiol.* (28): 1493–1504.
- Dynamax. 2007. Dynagage Sap Flow Sensor User Manual. 1–107. Last access on March 5th 2015.
- Effendi, R., S.B. Priyanto, M. Aqil, and M. Azrai. 2019. Drought adaptation level of maize genotypes based on leaf rolling, temperature, relative moisture content, and grain yield parameters. *IOP Conf. Ser. Earth Environ. Sci.* 270(1). doi: 10.1088/1755-1315/270/1/012016.
- Fang, J., and Y. Su. 2019. Effects of Soils and Irrigation Volume on Maize Yield, Irrigation Water Productivity, and Nitrogen Uptake. *Sci. Rep.* 9(1): 1–11. doi: 10.1038/s41598-019-41447-z.
- Frensch, J., and E. Steudle. 1989. Axial and Radial Hydraulic Resistance to Roots of Maize (*Zea mays* L.). *Plant Physiol.* 91: 719–726.
- Gallardo, M., J. Eastham, P.J. Gregory, and N.C. Turner. 1996. A comparison of plant hydraulic conductances in wheat and lupins. *J. Exp. Bot.* 47(295): 233–239. doi: 10.1093/jxb/47.2.233.
- Hochberg, U., F.E. Rockwell, N.M. Holbrook, and H. Cochard. 2018. Iso/Anisohydry: A Plant–Environment Interaction Rather Than a Simple Hydraulic Trait. *Trends Plant Sci.* 23(2): 112–120. doi: 10.1016/j.tplants.2017.11.002.
- Hopmans, J.W., and K.L. Bristow. 2002. Current Capabilities and Future Needs of Root Water and Nutrient Uptake Modeling. In: Sparks, D.L.B.T.-A. in A., editor, *Advances in Agronomy*. Academic Press. p. 103–183
- Hubbard, R.M., M.G. Ryan, V. Stiller, and J.S. Sperry. 2001. Stomatal conductance and photosynthesis vary linearly with plant hydraulic conductance in ponderosa pine. *Plant, Cell Environ.* 24(1): 113–121. doi: 10.1046/j.1365-3040.2001.00660.x.
- IPCC. 2022. Impacts, Adaptation, and Vulnerability. Working Group II Contribution to the IPCC Sixth Assessment Report of the Intergovernmental Panel on Climate Change.
- Jorda, H., M.A. Ahmed, M. Javaux, A. Carminati, P. Duddek, et al. 2022. Field scale plant water relation of maize (*Zea mays*) under drought – impact of root hairs and soil texture. *Plant Soil* 478(1–2): 59–84. doi: 10.1007/s11104-022-05685-x.
- Klein, T. 2014. The variability of stomatal sensitivity to leaf water potential across tree species indicates a continuum between isohydric and anisohydric behaviours. *Funct. Ecol.*: 1313–1320. doi: 10.1111/1365-2435.12289.
- Koehler, T., D.S. Moser, Á. Botezatu, T. Murugesan, S. Kaliamoorthy, et al. 2022. Going underground: soil hydraulic properties impacting maize responsiveness to water deficit. *Plant Soil* 478(1–2): 43–58. doi: 10.1007/s11104-022-05656-2.

- Lärm, L., F.M. Bauer, N. Hermes, J. van der Kruk, H. Vereecken, et al. 2023. Multi-year belowground data of minirhizotron facilities in Selhausen. *Sci. Data* 10(1): 1–15. doi: 10.1038/s41597-023-02570-9.
- Li, X., T.R. Sinclair, and L. Bagherzadi. 2016. Hydraulic Conductivity Changes in Soybean Plant-Soil System with Decreasing Soil Volumetric Water Content. *J. Crop Improv.* 30(6): 713–723. doi: 10.1080/15427528.2016.1231729.
- Li, Y., J.S. Sperry, and M. Shao. 2009. Hydraulic conductance and vulnerability to cavitation in corn (*Zea mays* L.) hybrids of differing drought resistance. *Environ. Exp. Bot.* 66(2): 341–346. doi: 10.1016/j.envexpbot.2009.02.001.
- Marin, M., D.S. Feeney, L.K. Brown, M. Naveed, S. Ruiz, et al. 2021. Significance of root hairs for plant performance under contrasting field conditions and water deficit. *Ann. Bot.* 128(1): 1–16. doi: 10.1093/aob/mcaa181.
- Meunier, F., A. Heymans, X. Draye, V. Couvreur, M. Javaux, et al. 2020. MARSHAL, a novel tool for virtual phenotyping of maize root system hydraulic architectures. *In Silico Plants* 2(1): 1–15. doi: 10.1093/insilicoplants/diz012.
- Meunier, F., M. Zarebanadkouki, M.A. Ahmed, A. Carminati, V. Couvreur, et al. 2018. Hydraulic conductivity of soil-grown lupine and maize unbranched roots and maize root-shoot junctions. *J. Plant Physiol.* 227(February): 31–44. doi: 10.1016/j.jplph.2017.12.019.
- Morandage, S., J. Vanderborght, M. Zörner, G. Cai, D. Leitner, et al. 2021. Root architecture development in stony soils. *Vadose Zo. J. (April)*: 1–17. doi: 10.1002/vzj2.20133.
- Müllers, Y., J.A. Postma, H. Poorter, and D. van Dusschoten. 2022. Stomatal conductance tracks soil-to-leaf hydraulic conductance in faba bean and maize during soil drying. *Plant Physiol.* doi: 10.1093/plphys/kiac422.
- Nguyen, T.H., M. Langensiepen, T. Gaiser, H. Webber, H. Ahrends, et al. 2022a. Responses of winter wheat and maize to varying soil moisture: From leaf to canopy. *Agric. For. Meteorol.* 314(December 2021): 108803. doi: 10.1016/j.agrformet.2021.108803.
- Nguyen, T.H., M. Langensiepen, H. Hueging, T. Gaiser, S.J. Seidel, et al. 2022b. Expansion and evaluation of two coupled root–shoot models in simulating CO₂ and H₂O fluxes and growth of maize. *Vadose Zo. J.* 21(3): 1–31. doi: 10.1002/vzj2.20181.
- Nguyen, T.H., M. Langensiepen, J. Vanderborght, H. Hüging, C.M. Mboh, et al. 2020. Comparison of root water uptake models in simulating CO₂ and H₂O fluxes and growth of wheat. *Hydrol. Earth Syst. Sci.* (24): 4943–4969. doi: 10.5194/hess-24-4943-2020.
- Ordóñez, R.A., S. V. Archontoulis, R. Martinez-Feria, J.L. Hatfield, E.E. Wright, et al. 2020. Root to shoot and carbon to nitrogen ratios of maize and soybean crops in the US Midwest. *Eur. J. Agron.* 120(June): 126130. doi: 10.1016/j.eja.2020.126130.
- Passioura, J.B., 2006. The perils of pot experiments. *Funct. Plant Biol.* 33 (12), 1075–1079. <https://doi.org/10.1071/FP06223>.
- Ranawana SRWMCJK, Siddique KHM, Palta JA et al (2021) Stomata coordinate with plant hydraulics to regulate transpiration response to vapour pressure deficit in wheat. *Functional Plant Biol* 48:839–850. <https://doi.org/10.1071/FP20392>
- Richards, R.A., G.J. Rebetzke, A.G. Condon, and A.F. van Herwaarden. 2002. Breeding Opportunities for

- Increasing the Efficiency of Water Use and Crop Yield in Temperate Cereals. *Crop Sci.* 42(1): 111–121. doi: 10.2135/cropsci2002.1110.
- Rodriguez-Dominguez, C.M., and T.J. Brodribb. 2019. Declining root water transport drives stomatal closure in olive under. *New Phytol.* 225: 126–134.
- Sinclair, T.R., and M.M. Ludlow. 1986. Influence of soil water supply on the plant water balance of four tropical grain legumes. *Aust. J. Plant Physiol.* 13: 329–341.
- Scharwies, J.D., and J.R. Dinneny. 2019. Water transport, perception, and response in plants. *J. Plant Res.* 132(3): 311–324. doi: 10.1007/s10265-019-01089-8.
- Schultz, H.R. 2003. Differences in hydraulic architecture account for near-isohydric and anisohydric behaviour of two field-grown *Vitis vinifera* L. cultivars during drought. *Plant, Cell Environ.* 26(8): 1393–1405. doi: 10.1046/j.1365-3040.2003.01064.x.
- Stadler, A., S. Rudolph, M. Kupisch, M. Langensiepen, J. van der Kruk, et al. 2015. Quantifying the effects of soil variability on crop growth using apparent soil electrical conductivity measurements. *Eur. J. Agron.* 64: 8–20. doi: 10.1016/j.eja.2014.12.004.
- Sulis, M., V. Couvreur, J. Keune, G. Cai, I. Trebs, et al. 2019. Incorporating a root water uptake model based on the hydraulic architecture approach in terrestrial systems simulations. *Agric. For. Meteorol.* 269–270: 28–45. doi: <https://doi.org/10.1016/j.agrformet.2019.01.034>.
- Sunita, C., T.R. Sinclair, C.D. Messina, and M. Cooper. 2014. Hydraulic conductance of maize hybrids differing in transpiration response to vapor pressure deficit. *Crop Sci.* 54(3): 1147–1152. doi: 10.2135/cropsci2013.05.0303.
- Tardieu, F., X. Draye, and M. Javaux. 2017. Root Water Uptake and Ideotypes of the Root System: Whole-Plant Controls Matter. *Vadose Zo. J.* 16(9): 0. doi: 10.2136/vzj2017.05.0107.
- Tardieu, F., and T. Simonneau. 1998. Variability among species of stomatal control under fluctuating soil water status and evaporative demand: modelling isohydric and anisohydric behaviours. *J. Exp. Bot.* 49(March): 419–432. doi: 10.1093/jxb/49.Special_Issue.419.
- Tardieu, F. 2016. Too many partners in root – shoot signals . Does hydraulics qualify as the only signal that feeds back over time for reliable stomatal. *New Phytol.* 212: 802–804.
- Trillo, N., and R.J. Fernández. 2005. Wheat plant hydraulic properties under prolonged experimental drought: Stronger decline in root-system conductance than in leaf area. *Plant Soil* 277(1–2): 277–284. doi: 10.1007/s11104-005-7493-5.
- Tsuda, M., and M.T. Tyree. 1997. Whole-plant hydraulic resistance and vulnerability segmentation in *Acer saccharinum*. *Tree Physiol.* (17): 351–357.
- Turner, N.C., E.D. Schulze, and T. Gollan. 1984. The responses of stomata and leaf gas exchange to vapour pressure deficits and soil water content - I. Species comparisons at high soil water contents. *Oecologia* 63(3): 338–342. doi: 10.1007/BF00390662.
- Tyree, M.T., E.L. Fiscus, S.D. Wullschleger, and M.A. Dixon. 1986. Detection of Xylem Cavitation in Corn under Field Conditions. *Plant Physiol.* 82(2): 597–599. doi: 10.1104/pp.82.2.597.
- Vadez, V. 2014. Root hydraulics : The forgotten side of roots in drought adaptation. *F. Crop. Res.* 165: 15–24.

- Vadez, V., S. Choudhary, J. Kholová, C.T. Hash, R. Srivastava, et al. 2021. Transpiration efficiency: Insights from comparisons of C4 cereal species. *J. Exp. Bot.* 72(14): 5221–5234. doi: 10.1093/jxb/erab251.
- Vanderborght, J., V. Couvreur, F. Meunier, A. Schnepf, H. Vereecken, et al. 2021. From hydraulic root architecture models to macroscopic representations of root hydraulics in soil water flow and land surface models. *Hydrol. Earth Syst. Sci.* 25(9): 4835–4860. doi: 10.5194/hess-25-4835-2021.
- Vanderborght, J., A. Graf, C. Steenpass, B. Scharnagl, N. Prolingheuer, et al. 2010. Within-Field Variability of Bare Soil Evaporation Θ on Derived from Eddy Covariance Measurements. *Vadose Zo. J.* 9: 943–954. doi: 10.2136/vzj2009.0159.
- Vereecken, H., A. Schnepf, J.W. Hopmans, M. Javaux, D. Or, et al. 2016. Modeling Soil Processes: Review, Key Challenges, and New Perspectives. *Vadose Zo. J.* 15(5): vzj2015.09.0131. doi: 10.2136/vzj2015.09.0131.
- Vetterlein, D., M. Phalempin, E. Lippold, S. Schlüter, S. Schreiter, et al. 2022. Root hairs matter at field scale for maize shoot growth and nutrient uptake, but root trait plasticity is primarily triggered by texture and drought. *Plant Soil* 478(1–2): 119–141. doi: 10.1007/s11104-022-05434-0.
- Vitale, L., P. Di Tommasi, C. Arena, A. Fierro, A. Virzo De Santo, et al. 2007. Effects of water stress on gas exchange of field grown *Zea mays* L. in Southern Italy: An analysis at canopy and leaf level. *Acta Physiol. Plant.* 29(4): 317–326. doi: 10.1007/s11738-007-0041-6.
- Wang, N., J. Gao, and S. Zhang. 2017. Overcompensation or limitation to photosynthesis and root hydraulic conductance altered by rehydration in seedlings of sorghum and maize. *Crop J.* 5(4): 337–344. doi: 10.1016/j.cj.2017.01.005.
- Weihermüller, L., Huisman, J. A., Lambot, S., Herbst, M., & Vereecken, H. (2007). Mapping the spatial variation of soil water content at the field scale with different ground penetrating radar techniques. *Journal of Hydrology*, 340, 205–216. <https://doi.org/10.1016/j.jhydrol.2007.04.013>
- Welcker, C., W. Sadok, G. Dignat, M. Renault, S. Salvi, et al. 2011. A common genetic determinism for sensitivities to soil water deficit and evaporative demand: Meta-analysis of quantitative trait loci and introgression lines of maize. *Plant Physiol.* 157(2): 718–729. doi: 10.1104/pp.111.176479.
- Zhuang, J., Y. Jin, and T. Miyazaki. 2001. ESTIMATING WATER RETENTION CHARACTERISTIC FROM SOIL PARTICLE-SIZE DISTRIBUTION USING A NON-SIMILAR MEDIA CONCEPT. *Soil Sci.* 166(5). https://journals.lww.com/soilsci/Fulltext/2001/05000/ESTIMATING_WATER_RETENTION_CHARACTERISTIC_FROM.2.aspx.
- Zwieniecki, M.A., P.J. Melcher, C.K. Boyce, L. Sack, and N.M. Holbrook. 2002. Hydraulic architecture of leaf venation in *Laurus nobilis* L. *Plant, Cell Environ.* 25(11): 1445–1450. doi: 10.1046/j.1365-3040.2002.00922.x.

Author contribution

Huu Thuy Nguyen, Thomas Gaiser, Jan Vanderborght, and Frank Ewert: Conceptualization; Huu Thuy Nguyen, and Hubert Hüging: Data curation and data quality check (aboveground measurements); Lena Lärm, Felix Bauer, Anja Klotzsche, Jan Vanderborght, and Andrea Schnepf: data curation and data quality check (belowground measurements); Huu Thuy Nguyen: Formal data analysis and visualization; Thomas Gaiser, Jan Vanderborght, Andrea Schnepf, and Frank Ewert: Funding acquisition & Project administration; Huu Thuy Nguyen: writing – original draft; all authors: review, editing, and finalizing the manuscript.

Competing interests

This manuscript has not been published and is not under consideration for publication in any other journal. All authors agreed and approved the manuscript and its submission to this journal. We declare there is no conflict of interest.

Code/Data availability

The meteorological data were collected from a weather station in Selhausen (Germany) which belongs to the TERENO network of terrestrial observatories. Weather data are freely available from the TERENO data portal (<https://www.tereno.net/ddp/dispatch?searchparams=freetext-Selhausen>, last access: October 2020) (TERENO, 2020). The data which were obtained from the minirhizotron facilities (under- and aboveground) are available from the corresponding author on reasonable requests.